

ARTICLE

T cell anergy in perinatal mice is promoted by T reg cells and prevented by IL-33

Jonatan Tuncel, Christophe Benoist, and Diane Mathis 

Perinatal T cells broadly access nonlymphoid tissues, where they are exposed to sessile tissue antigens. To probe the outcome of such encounters, we examined the defective elimination of self-reactive clones in Aire-deficient mice. Nonlymphoid tissues were sequentially seeded by distinct waves of CD4⁺ T cells. Early arrivers were mostly Foxp3⁺ regulatory T (T reg) cells and metabolically active, highly proliferative conventional T cells (T conv cells). T conv cells had unusually high expression of PD-1 and the IL-33 receptor ST2. As T conv cells accumulated in the tissue, they gradually lost expression of ST2, ceased to proliferate, and acquired an anergic phenotype. The transition from effector to anergic state was substantially faster in ST2-deficient perinates, whereas it was abrogated in IL-33–treated mice. A similar dampening of anergy occurred after depletion of perinatal T reg cells. Attenuation of anergy through PD-1 blockade or IL-33 administration promoted the immediate breakdown of tolerance and onset of multiorgan autoimmunity. Hence, regulating IL-33 availability may be critical in maintaining T cell anergy.

Introduction

Tolerance to self-antigens is enforced at several levels throughout the immune system (Xing and Hogquist, 2013). Ubiquitous antigens or antigens expressed at high concentrations promote deletion of cognate T cells as they differentiate in the thymus, whereas T cells that recognize rare antigens are more likely to escape thymic deletion and be controlled by peripheral tolerance mechanisms (McCaughy and Hogquist, 2008; Gascoigne and Palmer, 2011; Rudensky, 2011).

For the most part, adult naive T cells circulate between lymphatic organs, where they sample antigens delivered from nonlymphoid organs and the blood. In contrast, neonatal naive T cells broadly access nonlymphoid tissues, where they are exposed to sessile self-antigens (Alferink et al., 1998). Interactions between T cells and antigen-presenting cells during the perinatal period promote tolerance rather than activation. For example, allogeneic cell transfer and immunization with allogenic antigens at birth confer tolerance to reengraftment with the same cells (Billingham et al., 1953) or challenge with the same antigens (Hanan and Oyama, 1954; Gammon et al., 1986) in adulthood, demonstrating that T cell priming at birth can induce long-term tolerance of antigen-specific T cells. Moreover, failure to induce tolerance at birth has been associated with the development of autoimmunity or allergy later in life (Guerau-de-Arellano et al., 2009; Gollwitzer et al., 2014; Scharschmidt et al., 2015). Mice or humans deficient in the transcription factor

autoimmune regulator (Aire), which controls ectopic antigen expression in thymic medullary epithelial cells, develop autoimmunity in multiple organs as a result of diminished clonal deletion of self-reactive T cells and impaired regulatory T (T reg) cell differentiation (Anderson et al., 2002, 2005; Liston et al., 2003; Yang et al., 2015; Malchow et al., 2016). However, transgenic expression of Aire restricted to the first weeks of life is sufficient to correct the defects in T cell tolerance and, consequently, prevent the development of autoimmunity (Guerau-de-Arellano et al., 2009).

We recently explored several possible explanations for why Aire's presence is critical in perinates while being dispensable in adults (Yang et al., 2015). Neither the expression of Aire-induced genes nor the efficiency of clonal deletion was age dependent. Instead, Aire promoted the generation of a distinct population of T reg cells that, when transferred into perinatal Aire^{-/-} recipients, protected peripheral organs against autoimmune attack. The mechanisms underlying this protection and why it is a unique feature of perinatally derived T reg cells remain to be determined. Relatedly, T reg cell-mediated suppression during the first few weeks of life is critical for inducing tolerance against allergens and microbiota-derived antigens (Gollwitzer et al., 2014; Scharschmidt et al., 2015), suggesting that the path of at least some antigen-specific T cells is dictated at birth and influenced by perinatal T reg cells.

Department of Immunology, Harvard Medical School, Boston, MA.

Correspondence to Diane Mathis: cbdm@hms.harvard.edu; Christophe Benoist: cbdm@hms.harvard.edu.

© 2019 Tuncel et al. This article is distributed under the terms of an Attribution–Noncommercial–Share Alike–No Mirror Sites license for the first six months after the publication date (see <http://www.rupress.org/terms/>). After six months it is available under a Creative Commons License (Attribution–Noncommercial–Share Alike 4.0 International license, as described at <https://creativecommons.org/licenses/by-nc-sa/4.0/>).

Thus, there are several lines of evidence indicating that perinatal T reg cells play a critical role in the induction of T cell tolerance during the first weeks of life. However, the downstream mechanisms that enforce tolerance in perinatal T effector (T eff) cells are still poorly characterized, and what little is known derives almost entirely from studies on T eff cells circulating through lymphoid organs. Here, we addressed this matter by examining the dynamics and tolerization of peripheral CD4⁺ T cells in perinatal *Aire*^{+/+} and *Aire*^{-/-} mice, in particular cells within parenchymal tissues like the liver. The large number of organs targeted by autoimmunity in *Aire*^{-/-} mice and the bulk of evidence suggesting that the “Aire-less” disease is induced and driven by self-reactive CD4⁺ T cells (Devoss et al., 2008), with no or limited contribution from environmental factors (Gray et al., 2007), made this a particularly attractive model for this type of study.

Results

Nonlymphoid organs of perinatal *Aire*^{-/-} mice were enriched in effector/memory CD4⁺ T cells expressing high levels of programmed cell death 1 (PD-1)

To determine how Aire deficiency influenced the representation of T conventional (T conv) cells in nonlymphoid organs of perinates, we analyzed various organs of 8–10-d-old mice by flow cytometry. For example, CD4⁺ T conv cells were substantially more abundant in the liver of *Aire*^{-/-} than *Aire*^{+/+} littermates, whereas they were equally represented in the spleen of the two genotypes (Fig. 1 A). The majority of T conv cells in the liver of *Aire*^{-/-} mice, and a smaller proportion in the liver of *Aire*^{+/+} mice, had a CD44^{hi}CD62L^{lo} memory phenotype (Fig. 1 B). Several signaling and costimulatory receptors were up-regulated on CD44⁺ cells of the mutant mice, including GITR (glucocorticoid-induced TNF receptor family-related protein), ICOS (inducible costimulator), Lag3, and Tigit (Fig. S1 A). However, the marker whose overexpression was most striking in Aire-deficient cells was PD-1 (Fig. 1 C), an important costimulatory molecule with inhibitory functions (Lin et al., 2007). PD-1 was expressed on the majority of CD44⁺ T conv cells in the liver of *Aire*^{-/-} mice and on approximately half of the CD44⁺ T conv cells in *Aire*^{+/+} mice (Fig. 1 D). The proportions of PD-1⁺ T conv cells increased between days 4 and 10 after birth and thereafter decreased, dropping to splenic levels by day 20 (Fig. 1 E). Importantly, this was a true numerical decrease in PD-1⁺ cells, while both naive and CD44⁺PD-1⁻ T conv cell numbers remained relatively constant between days 10 and 20 (Fig. 1 F). The increased frequency of PD-1⁺ T conv cells was not confined to the liver; rather, it was evident in several, but not all, of the diverse tissues and organs examined in *Aire*^{-/-} mice (Fig. 1 G).

Similar to PD-1⁺ T conv cells, liver T reg cells increased both in frequency and number between days 5 and 10 and decreased between days 10 and 20 (Fig. 2, A and B). However, the T reg cell changes with age, unlike the T conv cell changes, were independent of Aire expression. On day 10 after birth, the frequency of T reg cells was increased in all nonlymphoid organs in comparison with the spleen (Fig. 2 C), again independent of Aire expression, and was highly correlated with the proportion of PD-1⁺ T conv cells in these tissues (Fig. 2 D).

In short, these results indicate that loss of Aire resulted in abnormal accumulations of activated T conv cells in many perinatal tissues. There was no evident relation as to whether or not an organ is targeted in Aire-deficient mice on the same genetic background (Jiang et al., 2005). In addition, there was a concomitant increase in T reg cells in the presence or absence of Aire.

Dynamics of naive and activated CD4⁺ T cells in the perinatal liver

Next, we explored factors that might explain the striking accumulation of PD-1⁺ T conv and T reg cells in the perinatal liver. In theory, a given cell compartment could increase in size due to the arrival of new cells, cell division, greater retention, and/or reduced death.

Thymic output is the primary reason for the increase in peripheral T cells in the spleen and lymph nodes during the first weeks after birth (Modigliani et al., 1994; den Braber et al., 2012), but the importance of thymic output for the increase in T cells in nonlymphoid organs is unknown. To gauge the proportion of recent thymic emigrants in a peripheral organ, we performed intrathymic biotinylation on *Aire*^{-/-} mice of various ages and analyzed the representation of biotinylated cells in the liver 12 h thereafter. Such cells constituted the majority of naive (PD-1⁻) T conv, PD-1⁺ T conv and T reg cells in 2-d-old mice, but by 4.5 d, the frequency of labeled PD-1⁺ T conv and T reg cells had dropped to <5%, while biotinylated cells still contributed one third of the naive T conv cell compartment (Fig. 3 A). In a second approach, we employed *Kaede*/B6 transgenic mice, which ubiquitously express a photoconvertible reporter that switches from green to red light emission when exposed to a 405-nm laser (Tomura et al., 2008, 2010; Bromley et al., 2013). Light exposure of thymocytes in 4-d-old mice, followed by quantification of photoconverted cells in the liver 24 h later, demonstrated, again, that, at 5 d of age, only the naive T conv population had a substantial component of newly exported thymocytes (Fig. S1 B).

Thus, while thymic output contributed to the initial pool of naive T conv cells in the liver of perinatal mice, it had a negligible impact on the increase in PD-1⁺ T conv and T reg cells. Instead, these cells increased through proliferation: the frequency of dividing CD4⁺ T cells, as measured by EdU incorporation at various time points after birth, was four- to sixfold higher for PD-1⁺ T conv and T reg cells than for naive T conv cells (Fig. 3 B). However, the proliferation of PD-1⁺ T conv and T reg cells was not the only reason for their increase. Both of these cell types were retained longer in the liver than were naive T conv cells, as demonstrated by photoconverting *Kaede*/B6 liver cells and measuring their representation at various time points thereafter (Fig. 3 C).

The number of PD-1⁺ T conv cells in the liver started to decline 10 d after birth, whereas naive T conv cell numbers remained unchanged (Fig. 1 E). Cell viability analysis of T conv cells in *Aire*^{-/-} mice revealed that the decline in PD-1⁺ T conv cells in the liver might, at least in part, have been related to their poor viability, as indicated by their higher levels of Annexin V/7AAD compared with those of PD-1⁻ T conv cells (Fig. 3 D).

In summary, a higher proliferation rate and more limited tissue egress explained the accumulation of PD-1⁺ T conv and T

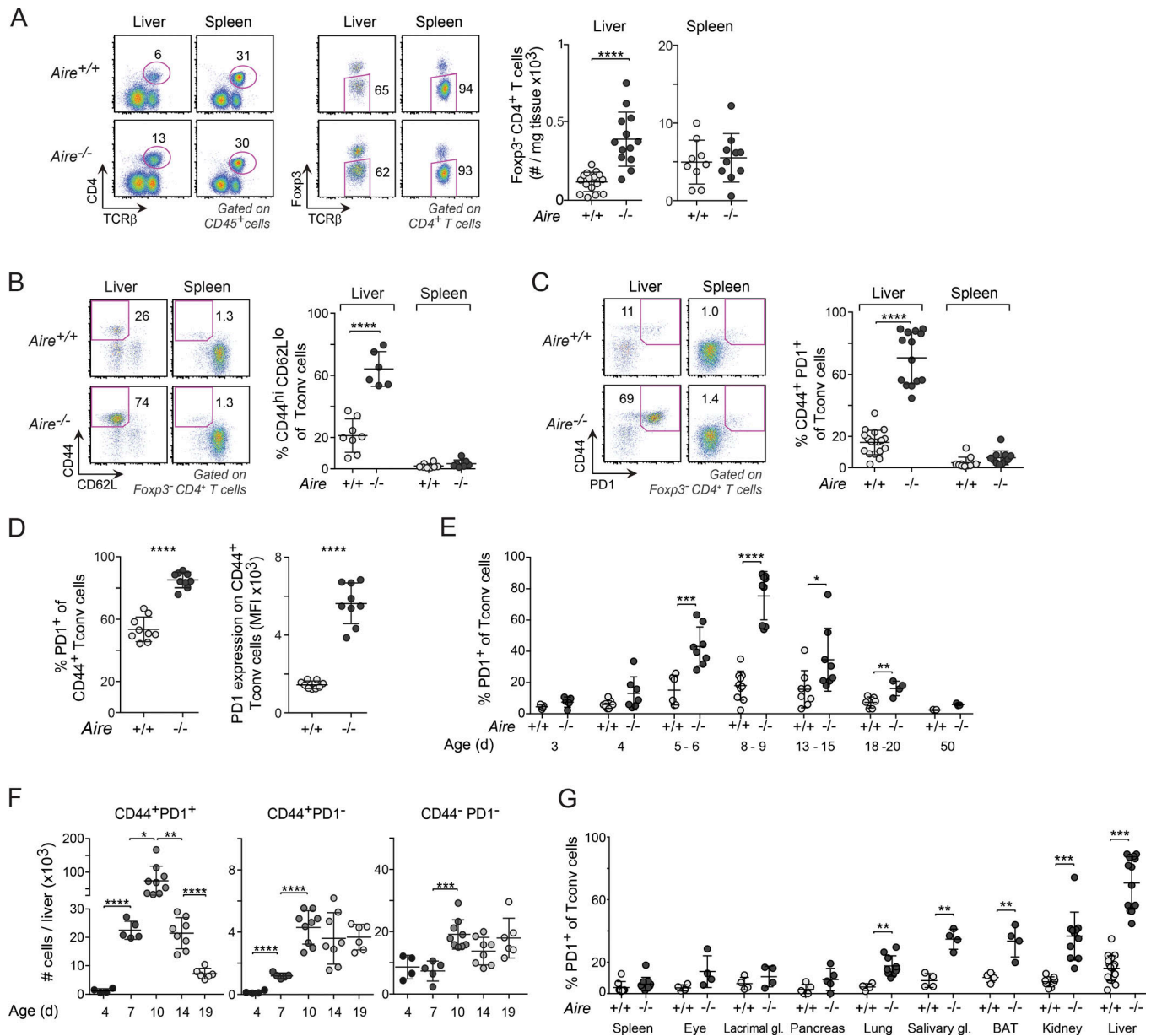


Figure 1. PD-1⁺CD4⁺ T conv cells were enriched in nonlymphoid organs of *Aire*^{-/-} perinates. (A) Quantification of Fcpx3⁻CD4⁺ T cells from the liver and spleen of 8–10-d-old mice (*n* = 9–16 mice/group). (B and C) Frequency of CD44^{hi}CD62L^{lo} (B) and CD44⁺PD-1⁺ (C) T conv cells from liver and spleen of 8–10-d-old mice. (D) Frequency of PD-1⁺ cells (left) and PD-1 mean fluorescence intensity (MFI; right) from the liver of 8–10-d-old *Aire*^{-/-} mice (*n* = 9 mice/group). (E) Frequency of PD-1⁺ T conv cells from liver of mice of various ages (*n* = 3–8 mice/group). (F) Numbers of T eff cells and naive T conv cells in the liver of differently aged *Aire*^{-/-} mice (*n* = 4–9 mice/group). (G) Frequency of PD-1⁺ T conv cells in the spleen and various nonlymphoid organs of 8–10-d-old mice (*n* = 4–16 mice/group). Representative flow cytometric plots in A–C show the gating strategy. Data are pooled from at least two independent experiments. Summary data (all panels) show mean ± SD. *, *P* ≤ 0.05; **, *P* ≤ 0.01; ***, *P* ≤ 0.001; ****, *P* ≤ 0.0001 (two-tailed unpaired Student's *t* test).

reg cells vis-à-vis naive T conv cells in the liver of *Aire*^{-/-} mice. Differential thymic output was not a major factor.

Age-related changes in the metabolic state, cytokine production, and activation of perinatal PD-1⁺ T conv cells in the liver

To generate mechanistic leads on the origin of this intriguing population of PD-1⁺CD4⁺ T conv cells, we sorted Fcpx3⁻PD-1⁻ and Fcpx3⁻PD-1⁺ CD4⁺ T cells from the liver of 5-d-old *Aire*^{-/-} mice

and analyzed their transcriptomes by RNA sequencing (RNA-seq). They proved very different, with ~4,000 genes differentially expressed twofold or more in the two cell states (Fig. 4 A, left). Gene-set enrichment analysis (GSEA) revealed up-regulation in PD-1⁺ cells of several pathways that control cell-cycle progression (e.g., G2/M, E2F, c-Myc, and K-Ras), consistent with the higher proliferation rate of these cells (Fig. 3 B), and pathways related to immune functions (e.g., IL-2/STAT5 and IL-6/JAK/STAT3; Fig. 4 A, right). In addition, PD-1⁺ cells

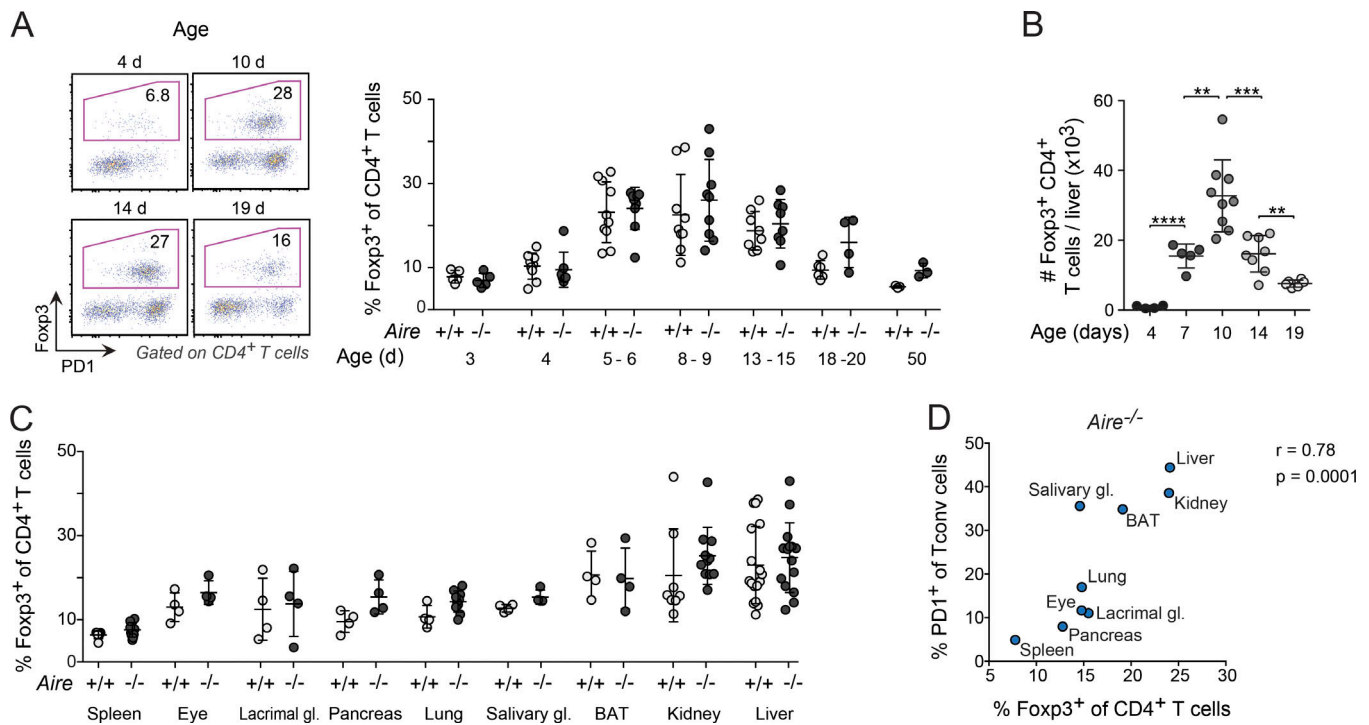


Figure 2. Nonlymphoid organs with high abundances of PD-1⁺ T conv cells were enriched in T reg cells. (A) Representative flow cytometric plots and summary data concerning T reg cell percentage at various ages ($n = 3-9$ mice/group). (B) Number of T reg cells in the liver of differently aged *Aire*^{-/-} mice ($n = 4-9$ mice/group). (C) Frequency of T reg cells in the spleen and various nonlymphoid organs of 8-10-d-old mice ($n = 4-16$ mice/group). (D) Correlation between frequencies of T reg cells (x axis) and PD-1⁺ T conv cells (y axis) in organs of 8-10-d-old *Aire*^{-/-} mice (median values of data shown in Figs. 1 G and 2 C; $n = 4-16$ mice/group). Data are pooled from two to four independent experiments and show mean \pm SD. Statistical analyses in A-C as in Fig. 1. **, $P \leq 0.01$; ***, $P \leq 0.001$.

were enriched in transcripts encoding members of metabolic pathways, such as the mTOR-AKT signaling pathway (mTORC1), which regulates aerobic glycolysis, and glucose transporters and glycolytic enzymes, e.g., GLUT1 (*Slc2A1*), triosephosphate isomerase 1 (*Tpi1*), and hexokinase (*Hk2*; Fig. 4 A).

PD-1⁺ cells were also enriched in transcripts overrepresented in activated T cells (Fig. 4 B), including a number encoding cytokines or their receptors, some of which were confirmed by flow cytometry (Fig. S1 C). However, they also shared the typical “exhaustion” profile of CD4⁺ T cells from mice chronically infected with lymphocytic choriomeningitis virus (Crawford et al., 2014; Fig. 4 B). While exhaustion is typically used to describe the progressive loss of T cell effector functions that occurs over several weeks of antigen stimulation, the transcriptionally related condition, anergy, usually occurs more rapidly (Schietinger and Greenberg, 2014; Wherry and Kurachi, 2015). Indeed, several “core” anergy-associated transcripts (e.g., *Rnfl28* and *FasI*; Rengarajan et al., 2000; Heissmeyer et al., 2004) were enriched in PD-1⁺ cells as well (Fig. 4 B).

PD-1 expression was up-regulated soon after T cells accessed the liver in perinatal mice and remained high for at least 7-8 d thereafter (Fig. 3 A). To compare the phenotypes of cells with short- versus long-term PD-1 up-regulation, we performed RNA-seq analysis on PD-1⁺ cells from 5- and 10-d-old mice. The transcriptome underwent substantial evolution during this time window with >2,000 transcripts up- or down-regulated at least twofold (Fig. 4 C, left). GSEA and signature analyses revealed

that several of the metabolic and cell-cycle pathways up-regulated in 5-d-old mice (*G2/M*, *Myc*, oxidative phosphorylation, mTORC1, and glycolysis) were less enriched on day 10 (Fig. 4 C, right). In addition, PD-1⁺ cells from 10-d-old mice appeared to be less activated, although transcripts associated with anergy and exhaustion remained at high levels (Fig. 4 D). Transcripts encoding several core proteins implicated in exhaustion and anergy (e.g., *Havcr2*, *Lag3*, *Tigit*, and *Tnfrsf18*) were expressed at higher levels in 10- versus 5-d old mice (Fig. 4 D). Further, consistent with the notion that PD-1⁺ cells acquired anergic properties over time, transcript levels of *Il2* (Telander et al., 1999) were much reduced in 10-d-old mice, whereas other cytokine transcripts (e.g., *Ifng*, *Il21*, and *Il10*) were not (Fig. 4 D).

In brief, PD-1⁺ T conv cells showed signs of enhanced metabolic activity, activation, and exhaustion/anergy shortly after arrival in the liver. Within 5 d, they had down-regulated *Il2* transcripts, metabolic pathways, and the activation signature, whereas the expression of exhaustion- and anergy-associated transcripts had increased.

Perinatal T reg cells were required for the maintenance of anergy in PD-1⁺ T conv cells

The transcriptional profile of PD-1⁺ T conv cells suggested that anergy might be a mechanism for the induction of tolerance in perinatal effector T cells (Fig. 4, B and D). Several additional observations supported this notion. First, high cell-surface expression of CD73 (encoded by *Nt5e*) and folate receptor 4 (FR4;

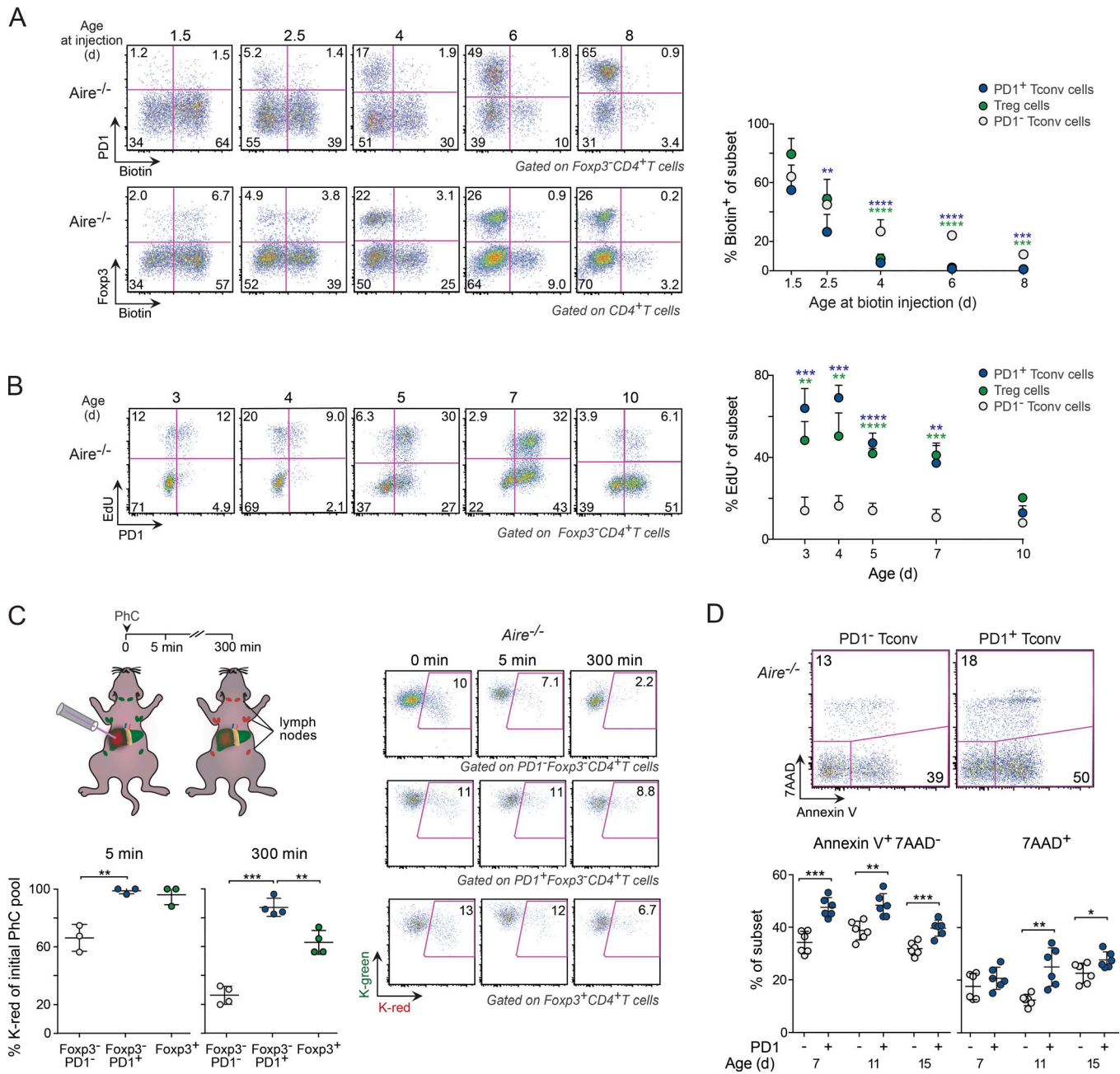


Figure 3. T cell dynamics in the perinatal liver. (A) Analysis of biotin-labeled CD4⁺ T conv cells in the liver 12 h after intrathymic injection of biotin ($n = 4-6$ mice/group). **(B)** Proliferation of liver CD4⁺ T cells in differently aged *Aire*^{-/-} perinates 4 h after EdU injection ($n = 5-7$ mice/group). **(C)** Frequency of photoconverted (PhC) CD4⁺ T cells (K-red) retained in the liver at various time points after light exposure of the organ in 6-d-old *Kaede/B6.Aire*^{-/-} mice ($n = 3-4$ mice/group). **(D)** Annexin V⁺ and 7AAD⁺ liver T conv cells in *Aire*^{-/-} mice of various ages ($n = 6$ mice/group). Data are pooled from two to four independent experiments and show mean \pm SD. Statistical analyses as in Fig. 1. *, $P \leq 0.05$; **, $P \leq 0.01$; ***, $P \leq 0.001$; ****, $P \leq 0.0001$.

encoded by *Izumotr*) distinguishes anergic cells in a polyclonal population (Kalekar et al., 2016), and transcripts encoding both of these markers were up-regulated in PD-1⁺ T conv cells from 10-d-old mice (Fig. 4 D). Accordingly, the proportion of CD73^{hi}FR4^{hi} among PD-1⁺ T conv cells in the liver of *Aire*^{-/-} mice increased eightfold between days 5 and 20 after birth but only fourfold in wild-type littermates (Fig. 5 A). Consistent with published data (Kalekar et al., 2016), the expression of *Nrp-1* and *Nur77* was much higher in anergic cells than in CD73^{lo}FR4^{lo}CD44⁺

(effector) T cells and was equally high or higher in anergic cells than in T reg cells (Fig. 5, B and C). Second, the expression of PD-1 was substantially higher in anergic cells than in T eff cells (Fig. S2 A), whereas their in vivo proliferation rate, as determined by EdU incorporation, was lower (Fig. S2 A). Thus, the liver microenvironment in perinates promoted an anergic phenotype in potentially self-reactive T cells.

Next, we sought to identify mechanisms involved in the induction of anergy in the tissue-localized PD-1⁺ T conv cells of

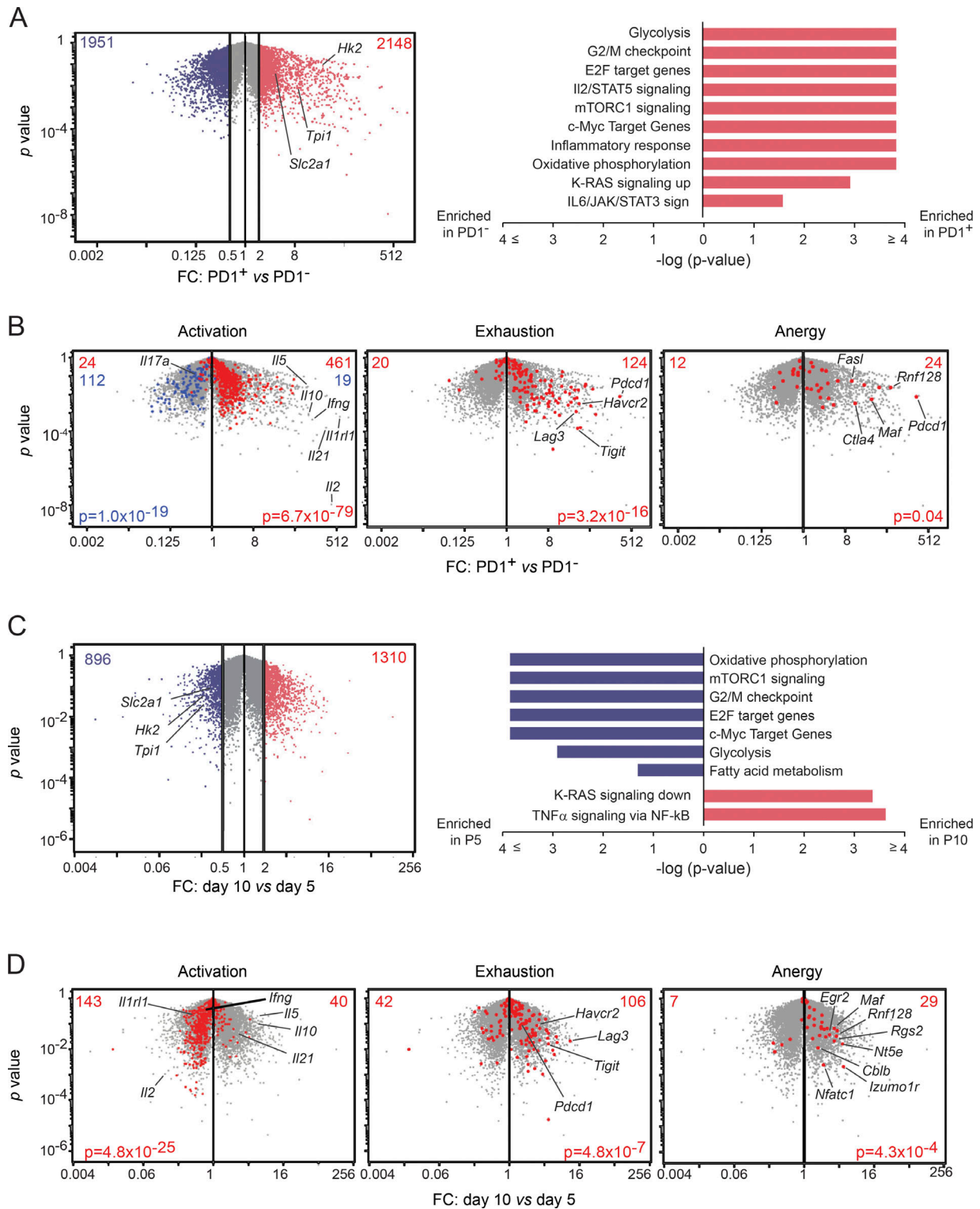


Figure 4. **Age-related changes in gene expression in perinatal PD-1⁺ T conv cells.** (A) RNA-seq analysis of PD-1⁺ and PD-1⁻ T conv cells from liver of 5-d-old *Aire*^{-/-} mice. Left: Volcano plot comparing transcriptomes from PD-1⁻ versus PD-1⁺ T conv cells. Genes at least twofold up- (red) or down- (blue) regulated. Right: GSEA using the Hallmark collection from the MSigDB. A selection of significantly enriched gene sets at false discovery rate <0.1. (B) Volcano plots of transcriptomes from PD-1⁻ versus PD-1⁺ T conv cells, as in A. Superimposed signatures (left to right): Activation up- (red) or down- (blue) signature from in vitro-activated T cells (Hill et al., 2007); exhaustion-up signature (transcripts overexpressed in exhausted vs. memory CD4⁺ T cells; Crawford et al., 2014); and anergy core signature (Macián et al., 2002; Zheng et al., 2012; Kalekar et al., 2016). FC, fold-change. (C) Left: Volcano plot comparing transcriptomes from PD-1⁺ T conv cells for 5- versus 10-d-old *Aire*^{-/-} mice. Right: GSEA Hallmark gene sets. (D) Volcano plots of transcriptomes from PD-1⁺ T conv cells in 5- versus 10-d-old *Aire*^{-/-} mice, as in C. Superimposed signatures are the same as in B. Data are pooled from two independent experiments ($n = 2$ mice/group/age).

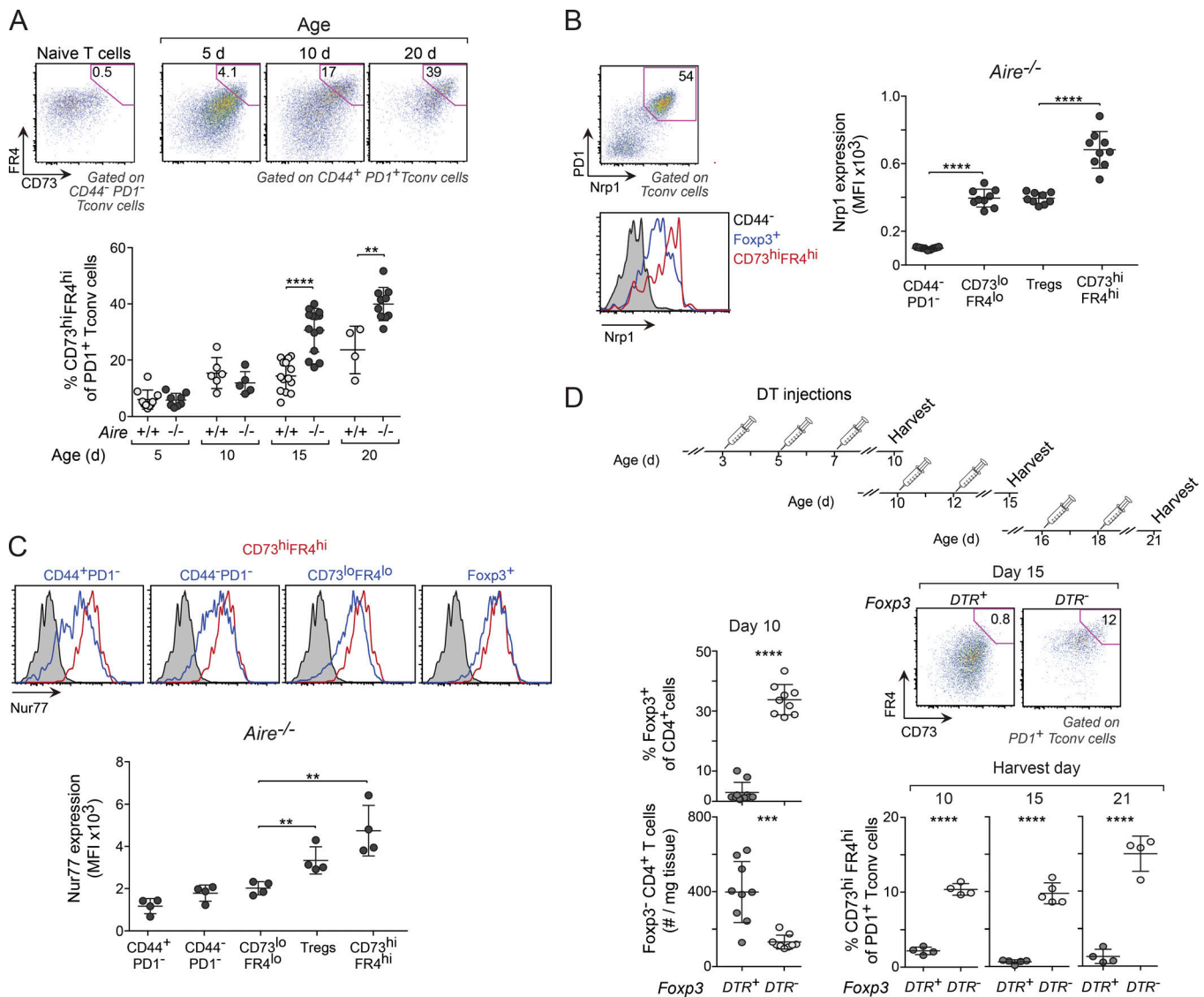


Figure 5. Perinatal T reg cells were critical for maintaining anergy in PD-1⁺ T conv cells. (A) Frequencies of anergic (CD73^{hi}FR4^{hi}) PD-1⁺ T conv cells in liver from mice of various ages. Top: Representative flow-cytometric plots showing gating strategy using CD44-PD-1⁺ T conv cells to identify anergic cells. Bottom: Summary data (n = 4–14 mice/group). (B) Nrp1 expression on various populations of liver CD4⁺ T cells from 10-d-old *Aire*^{-/-} mice (n = 9 mice/group). (C) Expression of Nur77 in cells from 10-d-old Nur77^{eGFP} reporter mice (n = 4 mice/group). Nur77^{eGFP}⁻ cells were used as controls in all histograms (gray shadings). MFI, mean fluorescence intensity. (D) Frequency of anergic T conv cells in T reg cell-depleted perinates. Top: Treatment regimen for DT injection. Bottom left: T conv and T reg cell summary data on DT-treated 10-d-old mice. Right: Representative flow-cytometry plots and summary data for anergic T conv cells from DT-treated mice (n = 4–9 mice/group). Data are pooled from two to four independent experiments and show mean ± SD. Statistical analyses as in Fig. 1. **, P ≤ 0.01; ***, P ≤ 0.001; ****, P ≤ 0.0001.

perinatal mice. T reg cells facilitate the induction of anergy in CD4⁺ T conv cells under lymphopenic conditions in vivo (Vanasek et al., 2006) and in CD8⁺ T cells in vitro (Maeda et al., 2014). To determine whether they were required for the accumulation of anergic cells in perinates, we depleted T reg cells by treating *Foxp3*^{DTR+} mice, in which expression of the diphtheria toxin receptor (DTR) is driven by endogenous *Foxp3* promoter/enhancer elements, with diphtheria toxin (DT) on days 3, 5, and 7 after birth (also *Foxp3*^{DTR-} controls; Fig. 5 D, top). By 3 d after the last injection, there was almost complete depletion of T reg cells in the *Foxp3*^{DTR+} mice, whereas T conv cell numbers were increased compared with controls (Fig. 5 D, left). More than 80%

of T conv cells in T reg-depleted mice expressed PD-1 (Fig. S2 B), but, in contrast to T conv cells in *Aire*^{-/-} mice, they included very few CD73^{hi}FR4^{hi} anergic cells (Fig. 5 D, bottom). These data indicated that the accumulation of anergic cells depended on T reg cells; however, they did not reveal whether T reg cells actually induced anergy or whether they were needed to maintain cells in an anergic state. To address this point, we treated groups of *Foxp3*^{DTR+} and *Foxp3*^{DTR-} mice with DT starting at either day 10 or 16 after birth, at which point anergy had already been established. Again, in both groups, depletion of T reg cells substantially reduced the frequency (Fig. 5 D, bottom) and total number (Fig. S2 C) of anergic cells and increased the number of T eff cells

(Fig. S2 C), indicating that T reg cells were required to maintain PD-1⁺ T conv cells in an anergic state. Consistently, PD-1⁺ T conv cells from T reg cell-depleted perinates demonstrated a more activated and less “anergic” phenotype than PD-1⁺ T conv cells from DT-treated *Aire*^{-/-} (*Foxp3*^{DTR-/-}) mice, as shown by their higher expression of ST2, CD69, ICOS, and IL-17A and lower expression of IL-10, Tigit, and PD-1 itself (Fig. S2 D), further demonstrating that these two PD-1⁺ states were functionally distinct.

To determine whether the ability of T reg cells to induce and maintain anergy was dependent on whether or not the mice expressed Aire, we transferred CD45.1⁺ T reg cells from *Aire*^{+/+} or *Aire*^{-/-} mice into T reg cell-depleted 8-d-old *Foxp3*^{DTR+} mice (Fig. 6 A). Compared with *Foxp3*^{DTR+} mice treated only with DT, DT-treated, T reg cell-reconstituted recipients had reduced numbers of T conv cells in the liver, regardless of whether or not the donors expressed Aire (Fig. 6 B). Moreover, while the expression of CD44 by T conv cells was similar for all T reg cell-depleted mice (Fig. S3 A), the proportions of anergic CD44⁺PD-1⁺ T conv cells (Fig. 6 C) and the expression of PD-1 on CD44⁺ T conv cells (Fig. 6 D) were increased in T reg cell-reconstituted recipients, again independent of whether or not the donors expressed Aire. Thus, both Aire-dependent and independent T reg cells were capable of inducing and maintaining T cell anergy.

While T reg cell reconstitution was sufficient to reestablish T cell anergy in T reg cell-depleted perinates, expanding the T reg cell population in the liver to levels that were two- to threefold higher than that of normal *Aire*^{+/+} mice, via injections of low doses of IL-2/anti-IL-2 mAb complexes (Boyman et al., 2006), did not increase the proportion of anergic T conv cells further (Fig. S3, B and C). This observation suggests that the existing T reg cell pool was sufficiently large to maintain T conv cells in an anergic state.

Taken together, these findings indicated that at least a portion of the effector T cells that accessed nonlymphoid organs in perinatal mice were anergized. The maintenance of anergy critically depended on T reg cells.

IL-33-ST2 signaling inhibited anergy in PD-1⁺ T conv cells

During the course of our studies, we noted that the receptor for IL-33, ST2 (encoded by *Il1rl1*), was much more highly expressed on PD-1⁺ than PD-1⁻ liver T conv cells and that it was down-regulated over time (Figs. 7 A, 4 C, and S4 A). To uncover what role ST2 signaling played in PD-1⁺ T conv cells, we generated B6. *Aire*^{-/-}*Il1rl1*^{-/-} double-knockout mice and analyzed their liver T cell compartments by flow cytometry. ST2 deficiency reduced the proportion of CD44⁺PD-1⁺ T conv cells, regardless of whether the mice expressed Aire (Fig. 7 B). More strikingly, however, was the impact of ST2 deficiency on the proportion and numbers of anergic cells in both *Aire*^{-/-} (Figs. 7 C and S4 B) and *Aire*^{+/+} (Fig. S4 C) mice; unexpectedly, in the absence of ST2, 40–80% of the CD44⁺PD-1⁺ T conv cells demonstrated an anergic phenotype by day 10 after birth, as compared with ~20% in its presence. Moreover, ST2 deficiency was associated with reduced proliferation in PD-1⁺ T conv cells, as determined by stimulating CellTrace violet-labeled liver CD4⁺ T cells from 6-d-old *Il1rl1*^{-/-} and *Il1rl1*^{+/+} (*Aire*^{-/-}) mice with αCD3/28 in vitro (Fig. 7 D). In

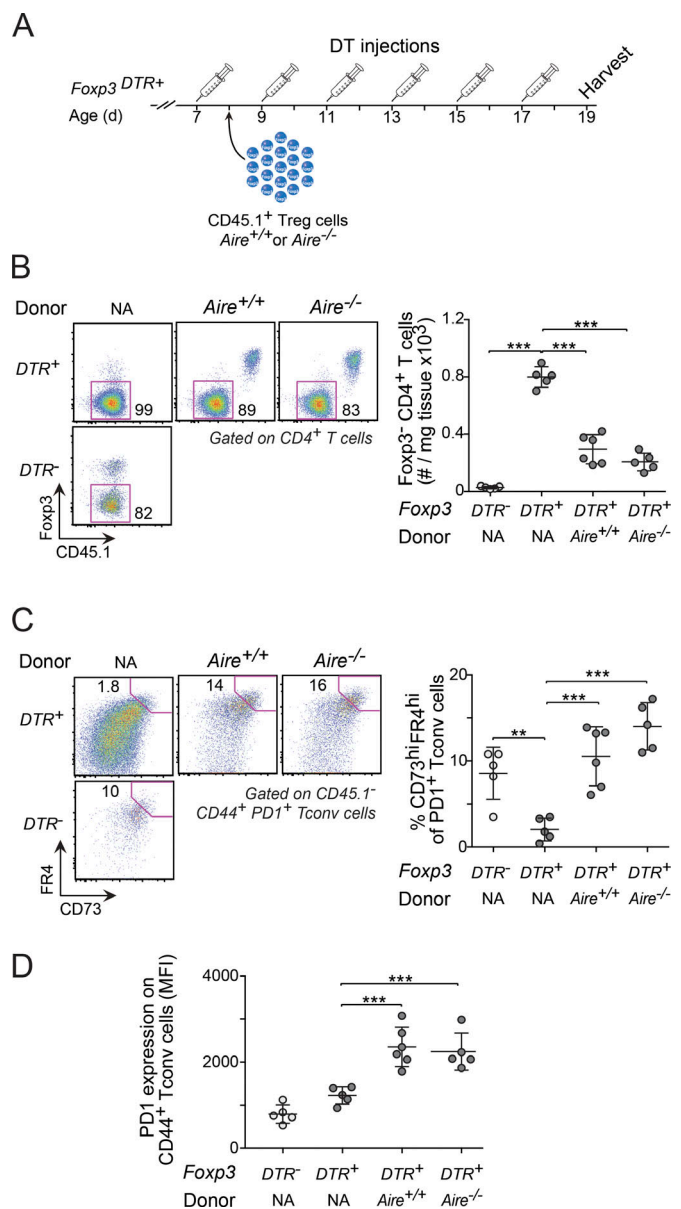


Figure 6. The ability of T reg cells to maintain anergy in effector cells was independent of Aire. (A) Regimen for adoptive T reg cell transfer and DT treatment. (B) Numbers of T conv cells in the liver of recipient mice and controls. (C and D) Frequency of anergic T conv cells (C) and expression of PD-1 on T conv cells (D). Data are pooled from two independent experiments (all panels, *n* = 5–6 mice/group) and show mean ± SD. Statistical analyses as in Fig. 1. MFI, mean fluorescence intensity; NA, not applicable. **, *P* ≤ 0.01; ***, *P* ≤ 0.001.

contrast, naive PD-1⁻ T conv cells in the liver and T conv cells in the spleen from the same mice showed no or only a modest difference in proliferation rate.

To further explore the association between ST2 and anergy, we treated *Aire*^{+/+} and *Aire*^{-/-} (*Il1rl1*^{+/+}) mice with recombinant IL-33 between days 4 and 8 or 8 and 16 after birth (Fig. 7 E). Consistent with the results from the *Il1rl1*^{-/-} mice, injection of rIL-33 between days 4 and 8 increased the frequency (Fig. 7 E) and number (Fig. S4 D) of CD44⁺PD-1⁺ T conv cells in 10-d-old *Aire*^{+/+} mice, with a trend toward higher frequencies in *Aire*^{-/-}

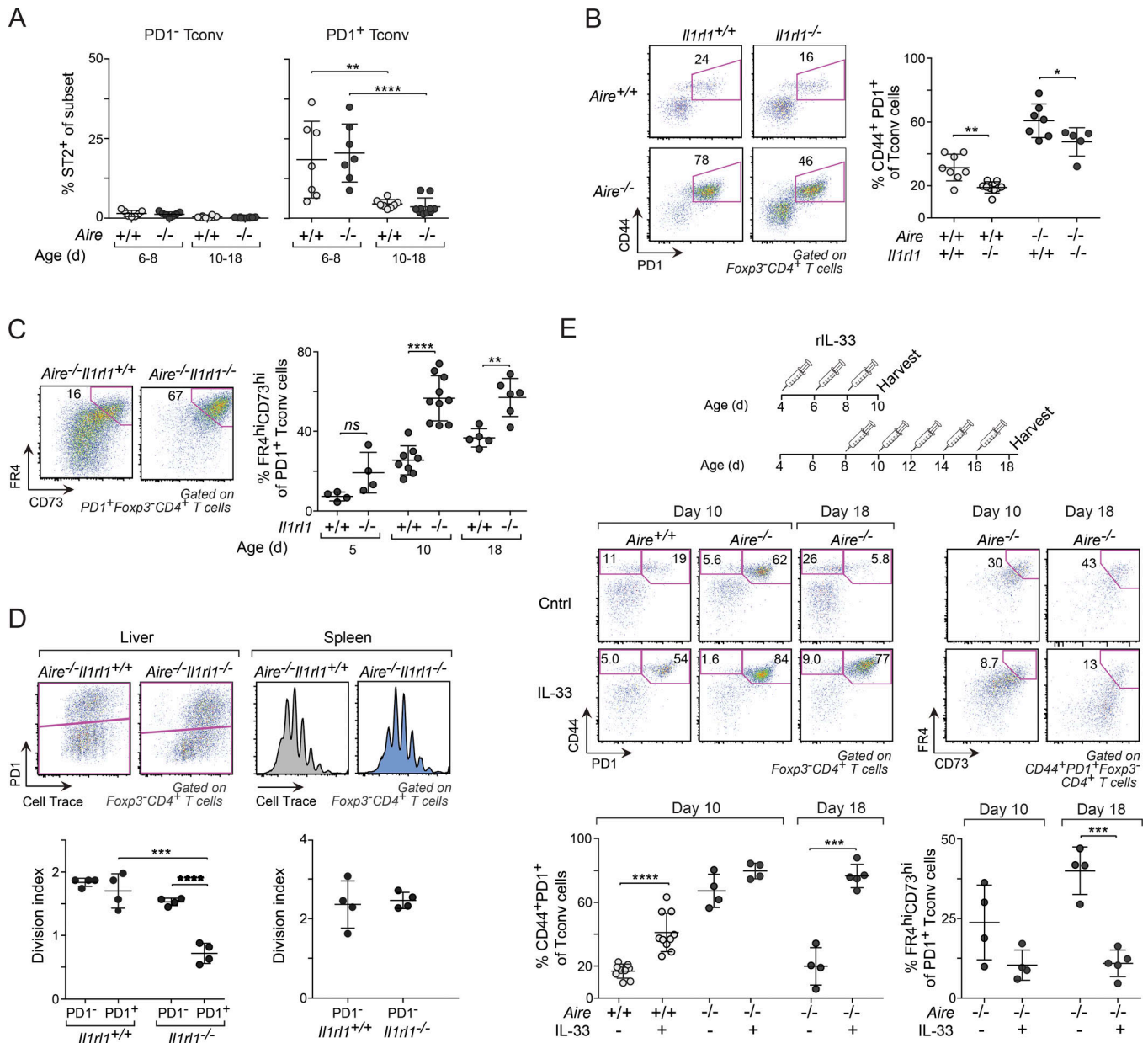


Figure 7. ST2 signaling reined in energy in perinatal liver T conv cells. (A) Frequency of ST2⁺ PD1⁻ and PD1⁺ T conv cells in liver from differently aged perinates ($n = 7-10$ mice/group; see Fig. S4 A for gating strategy of ST2⁺ cells). (B) CD44⁺PD1⁺ T conv cells from liver of 10-d-old mice ($n = 5-8$ mice/group). (C) Frequency of anergic (FR4^{hi}CD73^{hi}) PD1⁺ T conv cells in *Aire*^{-/-} mice of various ages ($n = 4-10$ mice/group). (D) Impact of ST2 deficiency on proliferation. α CD3/28 in vitro stimulation of sorted CellTrace violet-labeled liver and spleen CD4⁺ T cells from 6-d-old mice ($n = 4$ mice/group). (E) Frequency of total and anergic CD44⁺PD1⁺ T conv cells from liver of IL-33-treated mice. Top: Treatment regimen. Bottom: Representative flow-cytometric plots and summary data ($n = 4-10$ mice/group). Data are pooled from at least two independent experiments and show mean \pm SD. Statistical analyses as in Fig. 1. ns, not significant. *, $P \leq 0.05$; **, $P \leq 0.01$; ***, $P \leq 0.001$; ****, $P \leq 0.0001$.

mice as well. However, more important were the much-increased frequencies (Fig. 7 E) and numbers (Fig. S4 D) of CD44⁺PD1⁺ T conv cells in mice treated with rIL-33 between days 8 and 16 after birth. Furthermore, despite increasing the number of T reg cells (Fig. S4 E), late-perinatal treatment with rIL-33 reduced the levels of anergic cells in both *Aire*^{-/-} (Fig. 7 E) and *Aire*^{+/+} (Fig. S4 F) mice, while it increased the expression of ST2 on T conv cells (Fig. S4 G). Thus, high levels of IL-33 may prevent both the decline in CD44⁺PD1⁺ T conv cell numbers (Fig. 1 E) and the induction of anergy.

Given its potency at inhibiting anergy, regulating the bioavailability of IL-33 is likely to be of critical importance. To probe whether the levels of IL-33 were higher in nonlymphoid organs of *Aire*^{-/-} compared with *Aire*^{+/+} perinates, we measured the concentration of IL-33 in lysates from liver, kidney, lung, and spleen. While the levels of IL-33 varied substantially between the various tissues, its abundance was not dependent on whether or not the mice expressed Aire (Fig. 8 A). Since the bioavailability of IL-33 is likely to be regulated by ST2-expressing tissue-resident cells, in particular T reg cells

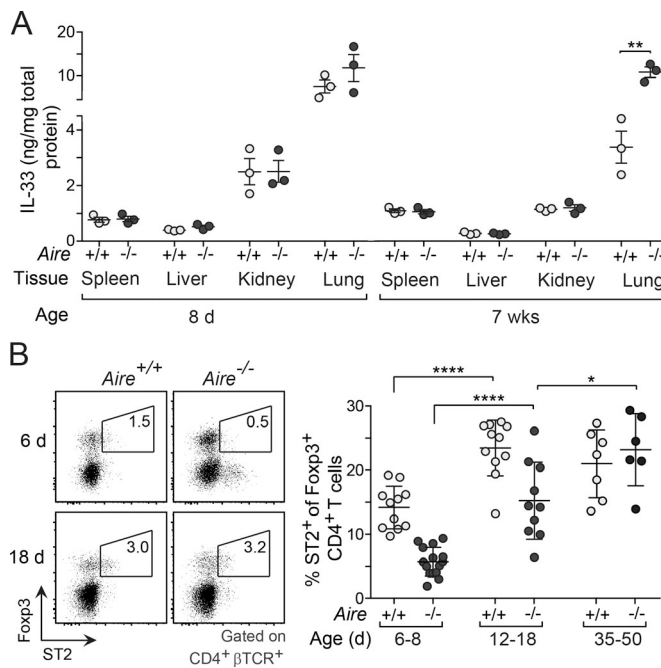


Figure 8. The expression of ST2 on T reg cells was age and Aire dependent. (A) Concentration of IL-33 protein in lysates from various tissues of perinatal and adult mice ($n = 3$ mice/group). (B) Frequency of ST2⁺ T reg cells in Aire^{+/+} and Aire^{-/-} mice of various ages. Left: Representative flow-cytometric plots. Right: Summary data ($n = 6$ –11 mice/group). Data are pooled from at least two independent experiments and show mean \pm SD. Statistical analyses as in Fig. 1. *, $P \leq 0.05$; **, $P \leq 0.01$; ****, $P \leq 0.0001$.

(Panduro et al., 2016), which were highly abundant in many of the perinatal tissues (Fig. 2 C), we compared the expression of ST2 between perinatal and adult T reg cells in the liver of Aire^{+/+} and Aire^{-/-} mice. In contrast to T conv cells (Fig. 7 A), the expression of ST2 on T reg cells was substantially lower in perinates than in adults, in particular in Aire^{-/-} mice, suggesting a higher bioavailability of IL-33 at birth and in the absence of Aire (Fig. 8 B).

In summary, these findings indicate that IL-33–ST2 signaling played an important role in warding off anergy in perinatal effector T cells. The expression of ST2 was lower on perinatal T reg cells than adult T reg cells in the liver, particularly in Aire^{-/-} mice, suggesting that the bioavailability of IL-33 in some tissues might be age dependent.

Energy reversal through PD-1 blockade or treatment with IL-33 induced early-onset autoimmunity in Aire-deficient mice

Disruption of the interaction between PD-1 and its ligands, PD-L1/L2, is associated with various autoimmune manifestations in both humans and mice (Nishimura et al., 1999; Salama et al., 2003; Hughes et al., 2015). In NOD mice, for example, PD-1 blockade leads to rapid onset of type 1 diabetes, both in adults and perinates (Ansari et al., 2003). Thus, an obvious question was whether such blockade could awaken potentially pathogenic T cell clones in Aire^{-/-} perinates. To address this question, we used NOD.Aire^{-/-} mice, which develop more widespread autoimmune disease than B6.Aire^{-/-} mice (Jiang et al., 2005). In prelude, we confirmed that the foundational observations on the

B6 background (i.e., the coordinate unusually high accumulations of PD-1⁺ T conv and T reg cells in several nonlymphoid organs of Aire^{-/-} perinates) held true on the NOD background (Fig. S5, A–D).

To determine whether inhibition of PD-1 could restore T cell proliferation, we treated NOD.Aire^{-/-} mice with an α PD-1 blocking mAb (versus an isotype-matched control mAb) between 8 and 14 d of age, followed by an injection of EdU on day 15 and analysis 4 h later. α PD-1 treatment enhanced the proliferation of CD44⁺CD73^{lo}FR4^{lo} effector T cells in all organs examined (Figs. 9 A and S5 E), whereas the proliferation of anergic T conv cells was increased in only some of them, and less strongly (Fig. S5 F). Accordingly, the frequencies of Foxp3⁺CD44⁺ T cells were significantly increased in all organs, and the total numbers of these cells were significantly increased in most of them (Fig. 9 B).

Next, we determined whether PD-1 blockade could accelerate the onset of autoimmunity in Aire^{-/-} perinates by injecting additional cohorts with α PD-1 or control mAbs using the protocol described above. α PD-1-treated Aire^{-/-} mice gained significantly less weight than either control-mAb-treated Aire^{-/-} mice or α PD-1-treated Aire^{+/+} littermates; by 20 d of age, they had lost so much weight that they had to be sacrificed (Fig. 9 C). PD-1 inhibition raised glucose levels and accelerated the onset of diabetes in Aire^{+/+} mice, consistent with published findings (Ansari et al., 2003), whereas it rendered Aire^{-/-} mice, which are diabetes resistant (Jiang et al., 2005; Niki et al., 2006), hypoglycemic (Fig. 9 C). To explore the cause of cachexia in α PD-1-treated Aire^{-/-} mice, we histologically examined several organs (Figs. 9 D and S5 G). Despite their young age (20–30 d), Aire^{-/-} mice treated with α PD-1 mAbs showed moderate to severe destruction and cellular infiltration of all of the organs typically affected in NOD.Aire^{-/-} mice except for the lacrimal glands and ovaries. Organs not typically affected in NOD.Aire^{-/-} mice (e.g., colon, kidney, and heart) did not respond to α PD-1 injection. Interestingly, similar levels of pneumonitis and prostatitis were observed in α PD-1-treated and control Aire^{-/-} mice, suggesting that not all self-reactive T cells were sufficiently anergized in the periphery at birth.

The accumulation of T eff cells in the liver of mice treated with α PD-1 closely resembled that of IL-33-treated mice (Fig. 7 E). Hypothesizing that treatment with IL-33 might also restore activation of pathogenic T cell clones, we treated NOD.Aire^{-/-} mice with recombinant IL-33 or vehicle (PBS) alone between days 8 and 16 after birth. Similar to Aire^{-/-} mice administered with α PD-1, IL-33-treated mice gained less weight than control-mAb-treated animals, and most developed mild hypoglycemia (Fig. S5 H). (Note that mice weighing $\geq 20\%$ less than controls were sacrificed [Fig. 9 E].) Histological examination of the pancreas, liver, lungs, and eyes revealed that all mice treated with IL-33 suffered from severe exocrine pancreatitis, hepatitis, and retinitis (Fig. 9 E and S5 I), although these conditions were milder than those of Aire^{-/-} mice treated with α PD-1 mAbs.

Thus, a broad spectrum of potentially pathogenic T cell clones was present in NOD.Aire^{-/-} mice at birth, but most of these were efficiently anergized, presumably reflecting contacts with self-antigens. The up-regulation of PD-1 and down-regulation of ST2 both contributed to reinforcing tolerance of these T cells.

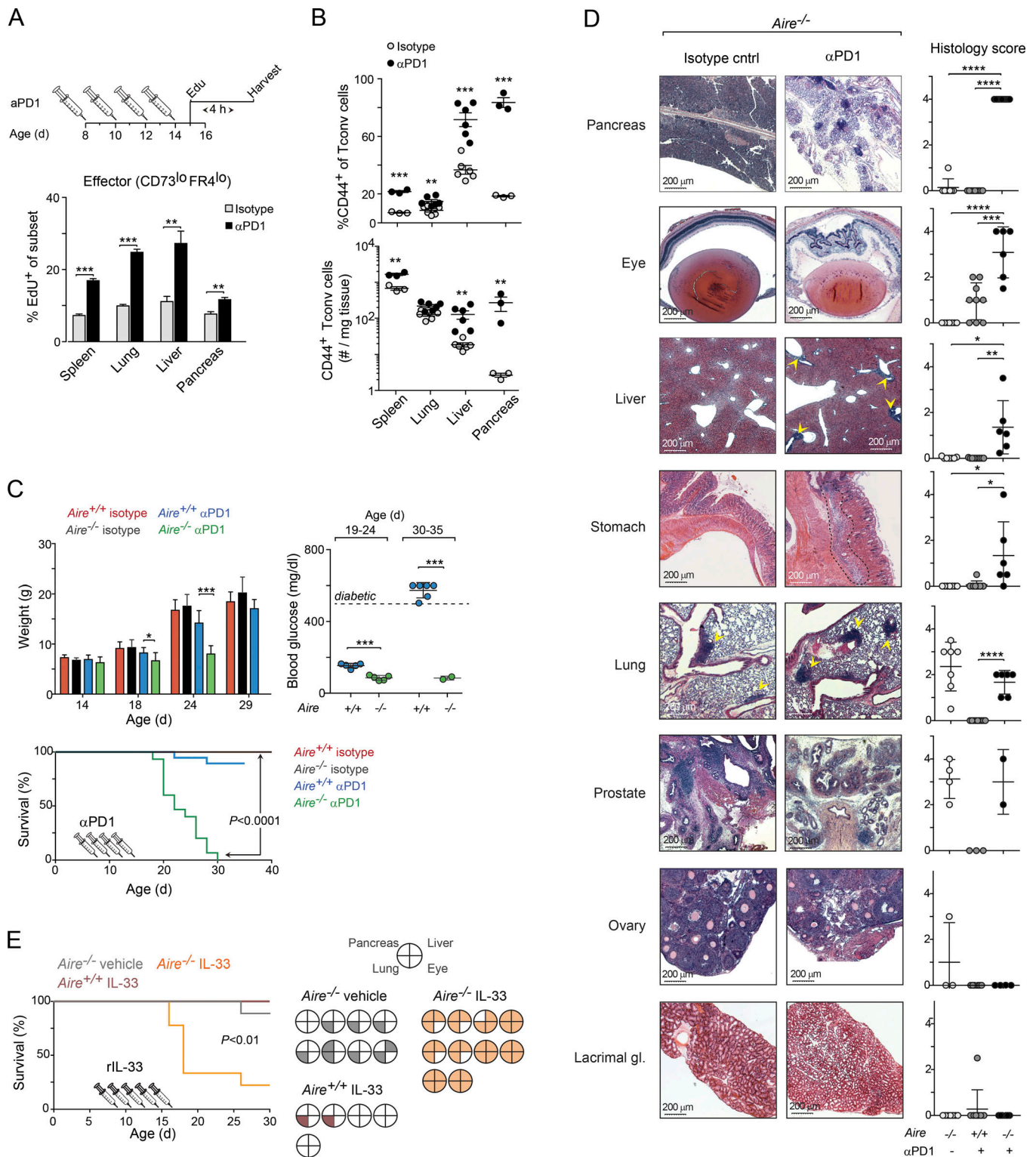


Figure 9. PD-1 inhibition or treatment with IL-33-induced early-onset autoimmunity in Aire-deficient NOD perinates. (A) Impact of αPD-1 treatment on T cell proliferation. Top: αPD-1 treatment regimen for data shown in A–D. Bottom: Summary of percentage of proliferating effector T cells in various organs 4 h after EdU injection ($n = 3\text{--}6$ mice/group; see Fig. S5 E for flow cytometric plots and corresponding data for anergic T conv cells). **(B)** Frequencies and numbers of CD44⁺ T conv cells from *Aire*^{-/-} mice ($n = 3\text{--}6$ mice/group). **(C)** Impact of αPD-1 treatment on autoimmune disease. Upper left: Weight change. Right: Blood-glucose levels, measured at two time points after mAb injection ($n = 5\text{--}6$ mice/group). Bottom: Survival curves ($n = 11\text{--}15$ mice/group); mice were sacrificed if their weight fell to <20% of that of control-treated littermates or if they developed diabetes. P value determined by log-rank (Mantel–Cox) test. **(D)** Histopathology analysis of organs from mice shown in C ($n = 6\text{--}9$ mice/group). Additional organs are shown in Fig. S5 G. Scale bars, 200 μm. **(E)** Impact of IL-33 treatment on autoimmune disease in NOD.*Aire*^{-/-} mice. Left: Survival curves ($n = 5\text{--}10$ mice/group). Right: Histopathology analysis at the time of death or end of the experiment (30 d after birth). Filled sections represent infiltrated tissues (see Fig. S8 C for histology scores). Data are pooled from at least two independent experiments and show mean ± SD. Statistical analyses as in Fig. 1. *, $P \leq 0.05$; **, $P \leq 0.01$; ***, $P \leq 0.001$; ****, $P \leq 0.0001$.

Discussion

Antigen priming during the perinatal window appears to favor tolerance of cognate T cells rather than their activation (Alferink et al., 1998). However, both the up- and downstream mechanisms that enforce such tolerance have remained elusive, particularly the events that unfold within parenchymal tissues as the initial wave of T cells enter and risk activation. Here, we showed that as newly exported T cells left the thymus and accessed peripheral nonlymphoid organs, transcriptional programs controlling activation and proliferation were broadly up-regulated. Two mechanisms were key for inducing or maintaining tolerance in these cells. First, T reg cells promoted an anergic state, and their absence during the perinatal window result in multiorgan autoimmunity (Kim et al., 2007). Second, IL-33 receptor signaling enhanced expansion of the liver T eff population, while inhibiting their anergy, and IL-33 augmentation perinatally also led to autoimmunity.

Treatment of perinatal *Aire*^{-/-} mice with α PD-1 mAb revealed that a surprisingly broad spectrum of potentially pathogenic T cells was present in *Aire*^{-/-} mice at birth and that PD-1 signaling in these cells was important to keep them in check. This observation is intriguing for several reasons. First, in newborn mice (1–3 d old), PD-1 was up-regulated on T conv cells as soon as they had entered the liver, most likely as the result of antigen stimulation (Honda et al., 2014). However, PD-1 up-regulation was not seen in older mice, indicating that self-reactive T cells might be preferentially enriched in early waves of thymic emigrants that access the tissues. This notion is consistent with previous findings that thymic emigrants are enriched in self-reactive cells in neonatal mice (Bonomo et al., 1994; He et al., 2013) and that early and late waves of perinatal T reg cells are functionally distinct (Scharschmidt et al., 2015; Yang et al., 2015). Importantly, PD-1 was up-regulated on T conv cells in most nonlymphoid organs but was barely detectable on their counterparts in the spleen and lymph nodes, which suggests that expression of PD-1 was not driven by the type of lymphopenia-induced proliferation known to occur during the early perinatal period (Min et al., 2003). Nor is it likely that the higher PD-1 expression on early versus late waves of perinatal cells reflect age-related differences in antigen presentation, given the well-known inferiority of neonatal antigen-presenting cells in priming naive T cells (Adkins et al., 2004; Dakic et al., 2004). Second, the amount of PD-1 expressed on T conv cells in the different organs did not correlate with how susceptible these organs were to autoimmune infiltration. Both kidney and liver T conv cells, for example, expressed high levels of PD-1, but only the liver showed signs of infiltration in mice treated with α PD-1 mAbs. Lastly, tolerance was not established in all organs; in perinatal prostate and lungs, infiltration was observed regardless of whether the mice had been treated with α PD-1 mAbs. Thus, there seem to be intrinsic differences between the organs, where some, such as the liver, have the capacity to tolerize thymic emigrants, whereas others do not have.

The fraction of CD44⁺PD-1⁺ T conv cells with an anergic CD73^{hi}FR4^{hi} phenotype increased with age, particularly in *Aire*^{-/-} mice. That these cells were anergic was supported by gene-expression profiling, which revealed that anergy-associated

transcripts accumulated in PD-1⁺ cells over time, and with published findings showing that anergic cells accumulate in the lymphoid organs of *Aire*-deficient mice, most prominently in aged mice (Kalekar et al., 2016). Most of the anergic cells in the perinatal liver probably derived from CD44⁺PD-1⁺ cells that had undergone multiple rounds of cell division, given the small number of anergic cells present in this organ before 5 d of age, rather than by a lack of costimulation during antigen priming (Schwartz, 1997, 2003). Phenotypically, anergic cells showed distinct differences vis-à-vis cells with an exhausted phenotype. Nur77, for example, whose expression is directly correlated with the amplitude and duration of TCR signaling (Baldwin and Hogquist, 2007; Moran et al., 2011; Ashouri and Weiss, 2017) and which is down-regulated in exhausted cells (Tinoco et al., 2016), was found to be up-regulated in anergic cells in both this study and a previous study (Kalekar et al., 2016). However, whether anergy, as classically defined, is the dominant mechanism behind the “dysfunctional” gene signature in perinatal PD-1⁺ T conv cells remains to be determined. The expression of transcripts associated with exhaustion (e.g., *Il10* and *Il21*; Brooks et al., 2006; Elsaesser et al., 2009), which is a state developing progressively from continuous antigen exposure (Wherry, 2011), increased over time in PD-1⁺ T conv cells as well. In addition, cells with an anergic CD73^{hi}FR4^{hi} phenotype constituted a minority of the CD44⁺PD-1⁺ population, and both anergic cells and cells with a CD73^{lo}FR4^{lo} phenotype were less proliferative in older perinates. Thus, it is possible that exhaustion and anergy developed in parallel, perhaps as distinct fractions of PD-1⁺ cells, or that they represented different stages of a common pathway.

Our results, in particular those concerning *Aire*^{-/-} mice treated with IL-33, suggest that the development of anergy is important for protection of organs against autoimmune infiltrations. Binding of IL-33 to its receptor, ST2, efficiently blocked and/or reversed the formation of anergy in these mice and promoted the expansion of T eff cells, resulting in autoimmune attacks on several nonlymphoid organs. In concert with these findings, T conv cells in ST2-deficient mice were more prone to become anergic. These novel findings on the relationship between ST2 and anergy raise several questions, one of the most important being whether IL-33 was affecting T conv cells directly by binding to ST2 on their surface or whether other ST2⁺ cells, such as T reg cells, innate lymphoid cells, or mast cells, were sensing IL-33 and, indirectly, contributed to the inhibition of anergy. Direct impact of IL-33 on T cell effector functions has previously been described for viral-specific CD8⁺ T cells (Bonilla et al., 2012), and, while it cannot be excluded that other ST2⁺ cells could have contributed to the inhibition of anergy, we were able to show that administration of IL-33 directly affected T conv cells by increasing their expression of ST2. In addition, the loss of ST2 expression on T conv cells coincided with the up-regulation of anergic markers on these cells, indicating that the level of ST2 expression on T conv cells correlated with their effector functions. Another question that warrants further discussion is whether the bioavailability of IL-33 is age dependent and influenced by the presence of *Aire* (or lack thereof). While the concentration of IL-33 in the analyzed tissues

was not dependent on whether or not the mice expressed Aire, the much lower expression of ST2 on perinatal compared with adult T reg cells, in particular in *Aire*^{-/-} mice, may suggest that IL-33 is more readily available to T conv cells during the perinatal period.

While signaling through the ST2 receptor helped maintain T conv cells in an effector state, T reg cells facilitated the induction, and were required for the maintenance, of anergy. Moreover, T reg cells were enriched in nonlymphoid organs with a high abundance of PD-1⁺ effector T cells, suggesting that T reg cell accumulation might be a direct consequence of the proliferation of these effector cells. The number of T reg cells in these organs, and the timing of their entry, seemed to be well adapted to maintaining tolerance and tissue homeostasis, as further increasing the size of the T reg cell compartment did not influence the size of the PD-1⁺ population, nor did it result in more anergic cells. In contrast, depletion of T reg cells in *Aire*^{+/+} mice resulted in a massive accumulation of T conv cells in the liver, the majority of which expressed high levels of PD-1 and ST2 as well as other molecules associated with enhanced effector functions. As mentioned above, these T conv cells did not become anergic, which may explain why T reg cell-deficient mice succumb to systemic autoimmunity and die at a young age (Chatila et al., 2000; Bennett et al., 2001; Brunkow et al., 2001; Kim et al., 2007). Several possible mechanisms might explain why T reg cells were required for the induction of anergy in perinates. For example, they express high levels of CD25, ST2, and other cytokine receptors and might, through sequestration of cytokines (Thornton and Shevach, 1998; Vignali et al., 2008), dampen proliferation and promote anergy.

As reported previously, perinatal T reg cells in *Aire*^{-/-} mice are functionally distinct from those found in *Aire*^{+/+} littermates; for example, the latter, but not the former, are able to suppress autoimmunity when transferred into *Aire*^{-/-} recipients. The differences between the genotypes are also reflected in the number of thymic and splenic T reg cells, both of which are higher in wild-type mice during the perinatal window. A possible explanation for these differences is that *Aire*^{-/-} mice lack an important subset of T reg cells that are dependent on Aire-controlled genes for their emergence. While such Aire-dependent T reg cells appear to be important to guard against an autoimmune attack later in life, both Aire-dependent and Aire-independent T reg cells were able to induce and maintain anergy in perinatal effector cells.

In brief, we have identified mechanisms that control anergy in nonlymphoid organs of perinatal mice and have shown that anergic cells arise in the presence of T reg cells and are particularly abundant in Aire-deficient mice. It is known that anergic cells can persist in the immune system over a long period of time and that, during this time, they maintain their ability to recognize antigens (Nossal and Pike, 1980). A gradual loss of T reg cell activity may revert these cells into effectors, which may explain why autoimmunity takes so long to develop.

Materials and methods

Mice

All mice used in this study were produced in our specific pathogen-free facilities at Harvard Medical School (HMS), and

the experiments were conducted under protocols approved by HMS's Institutional Animal Care and Use Committee. The following strains on B6 background were used: *Foxp3*-IRES-GFP mice were obtained from V. Kuchroo (Brigham and Women's Hospital, Boston, MA); the Kaede transgenic (tg) line (*Kaede*/B6) was obtained from O. Kanagawa (RIKEN, Wako, Japan; Tomura et al., 2008) and were crossed in-house to *Foxp3*^{Thy1.1} knock-in mice (from A. Rudensky, Memorial Sloan Kettering Cancer Center, New York, NY); *Nr4a1*^{EGFP} (*Nur77*^{GFP}) transgenic mice (Moran et al., 2011) were purchased from The Jackson Laboratory (#016671) and were crossed to *Foxp3*^{Thy1.1} mice; ST2-deficient mice (*Il1rl1*^{tm1Anjm}; Townsend et al., 2000) were obtained from A. McKenzie and R. Lee (Brigham and Women's Hospital, Boston, MA); and *Foxp3*-IRES-GFP-hDTR (*Foxp3*^{DTR}) mice were obtained from A. Rudensky. All mice, except those expressing *Foxp3*^{DTR}, were further bred with B6.*Aire*^{+/-} mice to generate F1 progenies that served as parents for the generation of *Aire*^{+/+} and *Aire*^{-/-} perinates. NOD.*Aire*^{-/-} and *Aire*^{+/+} mice (Jiang et al., 2005) were from our own colony at The Jackson Laboratory. All experiments were performed using sex-matched littermate controls.

Isolation of T cells from nonlymphoid tissues

Mice were anesthetized by isoflurane inhalation and perfused with ice-cold PBS containing 5 U/ml heparin through the left ventricle of the heart. All tissues, except brown adipose tissue, were excised, minced with scissors in DMEM (Thermo Fisher Scientific) containing collagenase IV (0.5 mg/ml; Gibco), DNase I (150 µg/ml; Sigma-Aldrich), FBS (1%), and 5 mM MgCl₂ and incubated in a 37°C water bath with shaking for 30–45 min. Digested tissues were passed through a 70-µm cell strainer and washed in DMEM/FBS. Leukocytes from perinatal liver were enriched by centrifugation at 60 × *g* for 1 min (without breaks), after which the pellet (containing mostly hepatocytes) was discarded. Remaining supernatant was centrifuged for 5 min at 1,500 rpm, and the pellet was resuspended in ACK lysis buffer (Lonza). Lysis was terminated by the addition of three volumes of staining buffer (FBS, DNase I, MgCl₂, and DMEM). Leukocytes from adult liver (>20 d of age) were enriched by Percoll (GE Healthcare) density centrifugation (40%:80%, 25 min at 1,126 × *g*). Brown adipose tissue leukocytes were prepared according to the same protocol as outlined above, except that collagenase II (1.5 mg/ml; Sigma-Aldrich) was used instead of collagenase IV and the digestion was shortened to 20 min.

Flow cytometry

The following antibodies were used for staining: anti-CD45 (30-F11), anti-CD4 (GK1.5), anti-TCRβ (H57-597), anti-CD44 (IM7), anti-PD-1 (29F.1A12), anti-CD62L (MEL-14), anti-FR4 (12A5), anti-CD73 (TY/11.8), anti-Nrp1 (3E12), anti-ICOS (C398.4A), anti-Tim3 (RMT3-23), anti-IFN-γ (XMG1.2), anti-IL-17A (TC11-18H10.1), and -CD69 (H1.2F3) from BioLegend; anti-ST2 (RMST2-2), anti-GITR (DTA-1), anti-Tigit (GIGD7), and anti-Foxp3 (FJK-16 s) from eBioscience; and anti-Lag3 (C9B7W) and IL-10 (JES3-9D7) from BD Pharmingen. Streptavidin-conjugated Brilliant Violet 605 or 786 (BioLegend) were used as secondary reagents. Cells were stained with a LIVE/DEAD Fixable dye

(Thermo Fisher Scientific), fixed in 1% paraformaldehyde (Electron Microscopy Sciences) for 10 min at room temperature, washed in staining buffer (1% FBS, 1 mM EDTA, and 0.02% NaN_3), and then stored in the same buffer until analyzed. For intracellular staining, cells were first incubated overnight at 4°C with a fixation and permeabilization buffer (eBioscience). For the detection of IFN- γ , IL-10, and IL-17A, cells were incubated in complete RPMI medium containing 50 $\mu\text{g}/\text{ml}$ phorbol-12-myristate-13-acetate and 1 mM ionomycin (both from Sigma-Aldrich) at 37°C for 4 h, the last 3 h in the presence of protein transport inhibitors (eBioscience). Click-iT EdU (Thermo Fisher Scientific) was used to measure proliferation of CD4⁺ T cells in vivo. Mice were administered i.p. with 0.15 mg (3–4 d old), 0.25 mg (5–7 d old), or 0.5 mg (10 d old) EdU (component A, reconstituted in PBS). Staining was performed using Pacific Blue-coupled azide following the manufacturer's instructions. For viability analysis, cells were stained with mAbs in the presence of phycoerythrin-labeled Annexin V and 7-Amino-Actinomycin D (BD Biosciences). Cells were acquired with an LSRII Fortessa or FACSymphony flow cytometer (both BD Biosciences), and data were analyzed using FlowJo software (Tree Star). For analysis of cell numbers, cells were stained with mAbs to CD45, TCR β , and CD4 (see above), after which CD4⁺ T cell counts were obtained on a MACSQuant analyzer (Miltenyi Biotech).

Cell migration analysis

For detection of thymic emigrants in the liver, a solution of 7 mg/ml sulfo-NHS-LC biotin (Pierce) was prepared in PBS immediately before the procedure. *Aire*^{-/-} perinates were anesthetized by induction of hypothermia (immersion in a slurry of ice and water for 10 min) and then placed on their backs on top of a closed ice-filled Petri dish under a dissecting microscope. A surgical incision was made through the skin along the midline from the top to the bottom of the sternum. Biotin was injected using a 0.3-ml insulin syringe (BD Ultrafine II, 31G) as follows: An approximate volume of 20 μl biotin solution was aspirated, and any trapped air was removed. Most of the solution was then expelled by applying light force onto the plunger, which left a residual volume of ~1.5–2 μl in the barrel that could be injected by applying more force to the plunger. The needle was inserted at a 30° angle, immediately below the second rib and adjacent to the sternum. The injections were performed with the bevel clearly visible through the connective tissue. After injection of each thymic lobe, the incision was closed with surgical tissue adhesive. The export of biotin-labeled thymocytes in the liver was determined after 12 h. Initial experiments were performed to confirm that only cells of thymic origin were biotin-labeled in the peripheral organs (data not shown). To ensure that biotinylation did not impact the functionality of thymocytes, we conducted a second, less invasive approach in which we photoconverted thymocytes in *Kaede*/B6 tg mice using violet light from a handheld laser (405 nm; peak power, <5 mW; sustained power, 0.5–4.9 mW; Laserglow Technologies). For photoconversion of cells in the liver, *Kaede*/B6 tg mice were anesthetized by an i.p. injection of ketamine (100 mg/kg; Parke Davis) and xylazine (10 mg/kg; Bayer). A 10-mm-long medial

incision was made through the abdominal wall to expose the liver, and violet light was shone onto the organ for a period of 2–3 min. The process was guided by a UV light source to ensure equal photoconversion of organs in all mice. Mice were euthanized by isoflurane inhalation immediately before photoconversion (time point, 0 min), after 5 min, or after 6 h.

Transcriptome analysis

Cells were sorted and processed according to the Immgen protocol for ultra-low-input RNA-seq analysis as described previously (Li et al., 2018). In brief, biological duplicates of 10³ DAPI-CD45⁺TCR β ⁺CD4⁺*Foxp3*^{GFP-} PD-1⁺ and PD-1⁻ cells from liver of 5- and 10-d-old B6.*Aire*^{-/-} perinates were double-sorted by Moflo into 5 μl of buffer TCL (Qiagen) containing 1% of 2-mercaptoethanol (Sigma-Aldrich). Smart-Seq2 library preparation and sequencing were performed as described previously (Li et al., 2018). Quantification of transcripts was performed using the Broad Technology Labs computational pipeline with Cuffquant version 2.2.1 (Trapnell et al., 2012). After normalization, reads were further filtered by minimal expression in Multiplot Studio (GenePattern; Broad Institute). Data analysis was performed using Multiplot Studio. GSEA was performed using GSEA 3.0 and the gene sets database Hallmark version 6.2. All signature gene sets are referenced in the corresponding figure legends. The sequencing data shown in this paper are available in the Gene Expression Omnibus under data repository accession no. GSE127882.

In vivo treatments

DT (D0564; Sigma-Aldrich) was injected i.p. into *Foxp3*^{DTR+} and *Foxp3*^{DTR-} littermates at 30 ng/g of body weight. The regimens for DT administration are depicted in the corresponding figure. For the adoptive transfer of T reg cells into *Foxp3*^{DTR+} perinates, 0.4 \times 10⁶ TCR β ⁺CD4⁺*Foxp3*⁺ cells from lymph nodes of 20- to 25-d-old *Aire*^{+/+} or *Aire*^{-/-} *Foxp3*-IRES-GFP mice were transferred into 8-d-old recipients. For the treatment of *Aire*^{+/+} mice with IL-2- α IL-2 mAb complexes, recombinant mouse IL-2 (PeproTech) was incubated with an α IL-2 mAb (JES6-1A12; BioLegend) at room temperature for 10 min before the injection. Mice were injected with 0.02 ml cytokine-antibody complexes containing 2.5 $\mu\text{g}/\text{ml}$ IL-2 and 82.5 $\mu\text{g}/\text{ml}$ α IL-2 mAb. Recombinant mouse IL-33 (BioLegend) was injected at 12.5 $\mu\text{g}/\text{kg}$; control mice were injected with an equal volume of PBS. α PD-1 mAb (29F.1A12) was injected at 3 mg/kg; control mice were injected with an equal amount of an isotype-matched control mAb (2A3; both from BioXCell). Measurement of blood glucose levels in mice treated with α PD-1 or IL-33 was performed on blood from the lateral tail vein.

In vitro cultures

For in vitro analysis of proliferating T conv cells, organs were excised and single-cell suspensions were prepared as described above. Cells were treated with ACK lysis buffer, stained with biotinylated mAbs to CD11b (M1/70; BioLegend), CD11c (N418; BioLegend), B220 (RA3-6B2; BD Pharmingen), CD8a (53-6.7; BioLegend), and F4/80 (BM8; BioLegend) for 8 min at room temperature, washed in sort buffer (FBS, DNase I, MgCl_2 , and

DMEM), and then incubated for 15 min at 4°C with Streptavidin-coupled magnetic beads (Dynal), followed by magnetic depletion of mAb-bound cells. The unbound fraction was stained with mAbs to CD45, TCR β , and CD4, and CD4⁺ T cells were sorted on a MoFlo Astrios (Beckman Coulter). Sorted cells were washed in PBS, stained with 1 μ M CellTrace violet (Thermo Fisher Scientific) at 37°C for 7 min with constant agitation, mixed with 10 volumes of complete RPMI medium, and stimulated with Dynabeads Mouse T-Activator CD3/CD28 bead (Thermo Fisher Scientific) at a 1:1 ratio for 96 h.

IL-33 ELISA

Approximately 20 mg of tissue from kidney, spleen, lung, and liver was homogenized in radioimmunoprecipitation assay buffer (Thermo Fisher Scientific) and then incubated at 4°C for 2 h. Lysates were cleared by centrifugation, and the protein concentration was determined using a detergent-compatible Bradford assay kit (Thermo Fisher Scientific). The concentration of IL-33 in the lysates was determined using the Legend Max Mouse IL-33 ELISA kit (BioLegend) according to the manufacturer's instructions.

Histology

Mice were anesthetized (with isoflurane) and perfused as described above. Tissues were collected and fixed at 4°C in Bouin's solution for 12–72 h (dependent on tissue) and then stored in 70% ethanol until processed. All tissues were processed at the Rodent Histopathology Core at HMS. Two sections per tissue were stained with hematoxylin and eosin for analysis. Images were acquired with a Nikon Ti or Keyence BZ microscope. Histology scorings were done blindly by two independent investigators. Averaged scores from the dual assessments were reported (scoring scale: 0, none; 1, mild; 2, mild to moderate; 3, moderate; 4, severe).

Statistical analysis

All statistical analyses were performed using GraphPad Prism software. If not stated otherwise, data are presented as mean \pm SD. Statistical significance, as indicated by asterisks, was determined by an unpaired *t* test (two-tailed) or a two-way ANOVA. *P* < 0.05 was considered significant (**, *P* < 0.01; ***, *P* < 0.001; ****, *P* < 0.0001). Volcano plot enrichment *P* values were determined using the χ^2 test.

Online supplemental material

Fig. S1 shows expression of various coreceptors by CD44⁺ and CD44⁻ T conv cells as well as photoconverted *Kaede*-tg recent thymic emigrants in perinatal liver and cytokine production by PD-1⁺ T conv cells in liver. Fig. S2 shows proportions of cycling anergic and effector T cells and their expression of PD-1, as well as the impact of T reg cell-depletion on the proportion of anergic and effector T cells and their expression of various coreceptors and cytokines. Fig. S3 shows frequency of liver CD44⁺ T conv cells after T reg cell-reconstitution in *Foxp3^{DTR+}* mice, as well as the impact of IL-2/anti-IL-2 treatment on anergic and effector T cells in liver. Fig. S4 shows the gating strategy of ST2⁺ T conv cells as well as the frequency of anergic, PD-1⁺, and ST2⁺

T conv cells in *Il1rl1^{-/-}* and IL-33-treated mice. Fig. S5 shows frequencies of PD-1⁺ T conv and T reg cells in various organs of NOD.*Aire^{+/+}* and NOD.*Aire^{-/-}* mice as well as the impact of PD-1 blockade on T cell proliferation and cellular infiltration in various tissues.

Acknowledgments

We thank K. Hattori, A. Rhoads, L. Yang, G. Buruzula, G. Gopalan, P. Montero Llopis, and C. Araneo for experimental support and C. Laplace for graphics.

Cell sorting was performed at the flow cores at HMS and Joslin Diabetes Center through National Institutes of Health grants P30DK036836 and S10OR021740. This work was funded by National Institutes of Health grant R01 DK060027 (to D. Mathis) and Swedish Research Council grant 2015-00364 (to J. Tuncel).

The authors declare no competing financial interests.

Author contributions: J. Tuncel, C. Benoist, and D. Mathis designed the study, interpreted data, and wrote the manuscript; J. Tuncel performed all experiments.

Submitted: 23 October 2018

Revised: 30 January 2019

Accepted: 22 March 2019

References

- Adkins, B., C. Leclerc, and S. Marshall-Clarke. 2004. Neonatal adaptive immunity comes of age. *Nat. Rev. Immunol.* 4:553–564. <https://doi.org/10.1038/nri1394>
- Alferink, J., A. Tafuri, D. Vestweber, R. Hallmann, G.J. Hämmerling, and B. Arnold. 1998. Control of neonatal tolerance to tissue antigens by peripheral T cell trafficking. *Science*. 282:1338–1341. <https://doi.org/10.1126/science.282.5392.1338>
- Anderson, M.S., E.S. Venanzi, L. Klein, Z. Chen, S.P. Berzins, S.J. Turley, H. von Boehmer, R. Bronson, A. Dierich, C. Benoist, and D. Mathis. 2002. Projection of an immunological self shadow within the thymus by the aire protein. *Science*. 298:1395–1401. <https://doi.org/10.1126/science.1075958>
- Anderson, M.S., E.S. Venanzi, Z. Chen, S.P. Berzins, C. Benoist, and D. Mathis. 2005. The cellular mechanism of Aire control of T cell tolerance. *Immunity*. 23:227–239. <https://doi.org/10.1016/j.immuni.2005.07.005>
- Ansari, M.J., A.D. Salama, T. Chitnis, R.N. Smith, H. Yagita, H. Akiba, T. Yamazaki, M. Azuma, H. Iwai, S.J. Khoury, et al. 2003. The programmed death-1 (PD-1) pathway regulates autoimmune diabetes in nonobese diabetic (NOD) mice. *J. Exp. Med.* 198:63–69. <https://doi.org/10.1084/jem.20022125>
- Ashouri, J.F., and A. Weiss. 2017. Endogenous Nur77 Is a Specific Indicator of Antigen Receptor Signaling in Human T and B Cells. *J. Immunol.* 198: 657–668. <https://doi.org/10.4049/jimmunol.1601301>
- Baldwin, T.A., and K.A. Hogquist. 2007. Transcriptional analysis of clonal deletion in vivo. *J. Immunol.* 179:837–844. <https://doi.org/10.4049/jimmunol.179.2.837>
- Bennett, C.L., J. Christie, F. Ramsdell, M.E. Brunkow, P.J. Ferguson, L. Whitesell, T.E. Kelly, F.T. Saulsbury, P.F. Chance, and H.D. Ochs. 2001. The immune dysregulation, polyendocrinopathy, enteropathy, X-linked syndrome (IPEX) is caused by mutations of FOXP3. *Nat. Genet.* 27:20–21. <https://doi.org/10.1038/83713>
- Billingham, R.E., L. Brent, and P.B. Medawar. 1953. Actively acquired tolerance of foreign cells. *Nature*. 172:603–606. <https://doi.org/10.1038/172603a0>
- Bonilla, W.V., A. Fröhlich, K. Senn, S. Kallert, M. Fernandez, S. Johnson, M. Kreuzfeldt, A.N. Hegazy, C. Schrick, P.G. Fallon, et al. 2012. The alarmin interleukin-33 drives protective antiviral CD8⁺ T cell responses. *Science*. 335:984–989. <https://doi.org/10.1126/science.1215418>

- Bonomo, A., P.J. Kehn, and E.M. Shevach. 1994. Premature escape of double-positive thymocytes to the periphery of young mice. Possible role in autoimmunity. *J. Immunol.* 152:1509–1514.
- Boyman, O., M. Kovar, M.P. Rubinstein, C.D. Surh, and J. Sprent. 2006. Selective stimulation of T cell subsets with antibody-cytokine immune complexes. *Science.* 311:1924–1927. <https://doi.org/10.1126/science.1122927>
- Bromley, S.K., S. Yan, M. Tomura, O. Kanagawa, and A.D. Luster. 2013. Recirculating memory T cells are a unique subset of CD4⁺ T cells with a distinct phenotype and migratory pattern. *J. Immunol.* 190:970–976. <https://doi.org/10.4049/jimmunol.1202805>
- Brooks, D.G., M.J. Trifilo, K.H. Edelmann, L. Teyton, D.B. McGavern, and M.B. Oldstone. 2006. Interleukin-10 determines viral clearance or persistence in vivo. *Nat. Med.* 12:1301–1309. <https://doi.org/10.1038/nm1492>
- Brunkow, M.E., E.W. Jeffery, K.A. Hjerrild, B. Paepfer, L.B. Clark, S.A. Yaszko, J.E. Wilkinson, D. Galas, S.F. Ziegler, and F. Ramsdell. 2001. Disruption of a new forkhead/winged-helix protein, scurf1, results in the fatal lymphoproliferative disorder of the scurfy mouse. *Nat. Genet.* 27:68–73. <https://doi.org/10.1038/83784>
- Chatila, T.A., F. Blaeser, N. Ho, H.M. Lederman, C. Voulgaropoulos, C. Helms, and A.M. Bowcock. 2000. JM2, encoding a fork head-related protein, is mutated in X-linked autoimmunity-allergic dysregulation syndrome. *J. Clin. Invest.* 106:R75–R81. <https://doi.org/10.1172/JCI11679>
- Crawford, A., J.M. Angelosanto, C. Kao, T.A. Doering, P.M. Odorizzi, B.E. Barnett, and E.J. Wherry. 2014. Molecular and transcriptional basis of CD4⁺ T cell dysfunction during chronic infection. *Immunity.* 40:289–302. <https://doi.org/10.1016/j.immuni.2014.01.005>
- Dakic, A., Q.X. Shao, A. D'Amico, M. O'Keefe, W.F. Chen, K. Shortman, and L. Wu. 2004. Development of the dendritic cell system during mouse ontogeny. *J. Immunol.* 172:1018–1027. <https://doi.org/10.4049/jimmunol.172.2.1018>
- den Braber, I., T. Mugwagwa, N. Vrisekoop, L. Westera, R. Mögling, A.B. de Boer, N. Willems, E.H. Schrijver, G. Spierenburg, K. Gaiser, et al. 2012. Maintenance of peripheral naive T cells is sustained by thymus output in mice but not humans. *Immunity.* 36:288–297. <https://doi.org/10.1016/j.immuni.2012.02.006>
- Devoss, J.J., A.K. Shum, K.P. Johannes, W. Lu, A.K. Krawisz, P. Wang, T. Yang, N.P. Leclair, C. Austin, E.C. Strauss, and M.S. Anderson. 2008. Effector mechanisms of the autoimmune syndrome in the murine model of autoimmune polyglandular syndrome type 1. *J. Immunol.* 181:4072–4079. <https://doi.org/10.4049/jimmunol.181.6.4072>
- Elsaesser, H., K. Sauer, and D.G. Brooks. 2009. IL-21 is required to control chronic viral infection. *Science.* 324:1569–1572. <https://doi.org/10.1126/science.1174182>
- Gammon, G., K. Dunn, N. Shastri, A. Oki, S. Wilbur, and E.E. Sercarz. 1986. Neonatal T-cell tolerance to minimal immunogenic peptides is caused by clonal inactivation. *Nature.* 319:413–415. <https://doi.org/10.1038/319413a0>
- Gascoigne, N.R., and E. Palmer. 2011. Signaling in thymic selection. *Curr. Opin. Immunol.* 23:207–212. <https://doi.org/10.1016/j.coi.2010.12.017>
- Gollwitzer, E.S., S. Saglani, A. Trompette, K. Yadava, R. Sherburn, K.D. McCoy, L.P. Nicod, C.M. Lloyd, and B.J. Marsland. 2014. Lung microbiota promotes tolerance to allergens in neonates via PD-L1. *Nat. Med.* 20:642–647. <https://doi.org/10.1038/nm.3568>
- Gray, D.H., I. Gavanescu, C. Benoist, and D. Mathis. 2007. Danger-free autoimmune disease in Aire-deficient mice. *Proc. Natl. Acad. Sci. USA.* 104:18193–18198. <https://doi.org/10.1073/pnas.0709160104>
- Guerau-de-Arellano, M., M. Martinic, C. Benoist, and D. Mathis. 2009. Neonatal tolerance revisited: a perinatal window for Aire control of autoimmunity. *J. Exp. Med.* 206:1245–1252. <https://doi.org/10.1084/jem.20090300>
- Hanan, R., and J. Oyama. 1954. Inhibition of antibody formation in mature rabbits by contact with the antigen at an early age. *J. Immunol.* 73:49–53.
- He, Q., Y.M. Morillon II, N.A. Spidale, C.J. Kroger, B. Liu, R.B. Sartor, B. Wang, and R. Tisch. 2013. Thymic development of autoreactive T cells in NOD mice is regulated in an age-dependent manner. *J. Immunol.* 191:5858–5866. <https://doi.org/10.4049/jimmunol.1302273>
- Heissmeyer, V., F. Macián, S.H. Im, R. Varma, S. Feske, K. Venuprasad, H. Gu, Y.C. Liu, M.L. Dustin, and A. Rao. 2004. Calcineurin imposes T cell unresponsiveness through targeted proteolysis of signaling proteins. *Nat. Immunol.* 5:255–265. <https://doi.org/10.1038/ni1047>
- Hill, J.A., M. Feuerer, K. Tash, S. Haxhinasto, J. Perez, R. Melamed, D. Mathis, and C. Benoist. 2007. Foxp3 transcription-factor-dependent and -independent regulation of the regulatory T cell transcriptional signature. *Immunity.* 27:786–800. <https://doi.org/10.1016/j.immuni.2007.09.010>
- Honda, T., J.G. Egen, T. Lämmermann, W. Kastnermüller, P. Torabi-Parizi, and R.N. Germain. 2014. Tuning of antigen sensitivity by T cell receptor-dependent negative feedback controls T cell effector function in inflamed tissues. *Immunity.* 40:235–247. <https://doi.org/10.1016/j.immuni.2013.11.017>
- Hughes, J., N. Vudattu, M. Sznol, S. Gettinger, H. Kluger, B. Lupsa, and K.C. Herold. 2015. Precipitation of autoimmune diabetes with anti-PD-1 immunotherapy. *Diabetes Care.* 38:e55–e57.
- Jiang, W., M.S. Anderson, R. Bronson, D. Mathis, and C. Benoist. 2005. Modifier loci condition autoimmunity provoked by Aire deficiency. *J. Exp. Med.* 202:805–815. <https://doi.org/10.1084/jem.20050693>
- Kalekar, L.A., S.E. Schmiel, S.L. Nandiwada, W.Y. Lam, L.O. Barsness, N. Zhang, G.L. Stritesky, D. Malhotra, K.E. Pauken, J.L. Linehan, et al. 2016. CD4⁽⁺⁾ T cell anergy prevents autoimmunity and generates regulatory T cell precursors. *Nat. Immunol.* 17:304–314. <https://doi.org/10.1038/ni.3331>
- Kim, J.M., J.P. Rasmussen, and A.Y. Rudensky. 2007. Regulatory T cells prevent catastrophic autoimmunity throughout the lifespan of mice. *Nat. Immunol.* 8:191–197. <https://doi.org/10.1038/ni1428>
- Li, C., J.R. DiSpirito, D. Zemmour, R.G. Spallanzani, W. Kuswanto, C. Benoist, and D. Mathis. 2018. TCR transgenic mice reveal stepwise, multi-site acquisition of the distinctive fat-Treg phenotype. *Cell.* 174:285–299.e12. <https://doi.org/10.1016/j.cell.2018.05.004>
- Lin, S.J., C.D. Peacock, K. Bahl, and R.M. Welsh. 2007. Programmed death-1 (PD-1) defines a transient and dysfunctional oligoclonal T cell population in acute homeostatic proliferation. *J. Exp. Med.* 204:2321–2333. <https://doi.org/10.1084/jem.20062150>
- Liston, A., S. Lesage, J. Wilson, L. Peltonen, and C.C. Goodnow. 2003. Aire regulates negative selection of organ-specific T cells. *Nat. Immunol.* 4:350–354. <https://doi.org/10.1038/ni906>
- Macián, F., F. García-Cózar, S.H. Im, H.F. Horton, M.C. Byrne, and A. Rao. 2002. Transcriptional mechanisms underlying lymphocyte tolerance. *Cell.* 109:719–731. [https://doi.org/10.1016/S0092-8674\(02\)00767-5](https://doi.org/10.1016/S0092-8674(02)00767-5)
- Maeda, Y., H. Nishikawa, D. Sugiyama, D. Ha, M. Hamaguchi, T. Saito, M. Nishioka, J.B. Wing, D. Adeegbe, I. Katayama, and S. Sakaguchi. 2014. Detection of self-reactive CD8⁺ T cells with an anergic phenotype in healthy individuals. *Science.* 346:1536–1540. <https://doi.org/10.1126/science.1229292>
- Malchow, S., D.S. Leventhal, V. Lee, S. Nishi, N.D. Socci, and P.A. Savage. 2016. Aire enforces immune tolerance by directing autoreactive T cells into the regulatory T cell lineage. *Immunity.* 44:1102–1113. <https://doi.org/10.1016/j.immuni.2016.02.009>
- McCaughey, T.M., and K.A. Hogquist. 2008. Central tolerance: what have we learned from mice? *Semin. Immunopathol.* 30:399–409. <https://doi.org/10.1007/s00281-008-0137-0>
- Min, B., R. McHugh, G.D. Sempowski, C. Mackall, G. Foucras, and W.E. Paul. 2003. Neonates support lymphopenia-induced proliferation. *Immunity.* 18:131–140. [https://doi.org/10.1016/S1074-7613\(02\)00508-3](https://doi.org/10.1016/S1074-7613(02)00508-3)
- Modigliani, Y., G. Coutinho, O. Buren-Defranoux, A. Coutinho, and A. Bandeira. 1994. Differential contribution of thymic outputs and peripheral expansion in the development of peripheral T cell pools. *Eur. J. Immunol.* 24:1223–1227. <https://doi.org/10.1002/eji.1830240533>
- Moran, A.E., K.L. Holzappel, Y. Xing, N.R. Cunningham, J.S. Maltzman, J. Punt, and K.A. Hogquist. 2011. T cell receptor signal strength in Treg and iNKT cell development demonstrated by a novel fluorescent reporter mouse. *J. Exp. Med.* 208:1279–1289. <https://doi.org/10.1084/jem.20110308>
- Niki, S., K. Oshikawa, Y. Mouri, F. Hirota, A. Matsushima, M. Yano, H. Han, Y. Bando, K. Izumi, M. Matsumoto, et al. 2006. Alteration of intrapancreatic target-organ specificity by abrogation of Aire in NOD mice. *J. Clin. Invest.* 116:1292–1301. <https://doi.org/10.1172/JCI26971>
- Nishimura, H., M. Nose, H. Hiai, N. Minato, and T. Honjo. 1999. Development of lupus-like autoimmune diseases by disruption of the PD-1 gene encoding an ITIM motif-carrying immunoreceptor. *Immunity.* 11:141–151. [https://doi.org/10.1016/S1074-7613\(00\)80089-8](https://doi.org/10.1016/S1074-7613(00)80089-8)
- Nossal, G.J., and B.L. Pike. 1980. Clonal anergy: persistence in tolerant mice of antigen-binding B lymphocytes incapable of responding to antigen or mitogen. *Proc. Natl. Acad. Sci. USA.* 77:1602–1606. <https://doi.org/10.1073/pnas.77.3.1602>
- Panduro, M., C. Benoist, and D. Mathis. 2016. Tissue Treas. *Annu. Rev. Immunol.* 34:609–633. <https://doi.org/10.1146/annurev-immunol-032712-095948>
- Rengarajan, J., P.R. Mittelstadt, H.W. Mages, A.J. Gerth, R.A. Kroczek, J.D. Ashwell, and L.H. Glimcher. 2000. Sequential involvement of NFAT and Egr transcription factors in FasL regulation. *Immunity.* 12:293–300. [https://doi.org/10.1016/S1074-7613\(00\)80182-X](https://doi.org/10.1016/S1074-7613(00)80182-X)

- Rudensky, A.Y. 2011. Regulatory T cells and Foxp3. *Immunol. Rev.* 241: 260–268. <https://doi.org/10.1111/j.1600-065X.2011.01018.x>
- Salama, A.D., T. Chitnis, J. Imitola, M.J. Ansari, H. Akiba, F. Tushima, M. Azuma, H. Yagita, M.H. Sayegh, and S.J. Khoury. 2003. Critical role of the programmed death-1 (PD-1) pathway in regulation of experimental autoimmune encephalomyelitis. *J. Exp. Med.* 198:71–78. <https://doi.org/10.1084/jem.20022119>
- Scharschmidt, T.C., K.S. Vasquez, H.A. Truong, S.V. Gearty, M.L. Pauli, A. Nosbaum, I.K. Gratz, M. Otto, J.J. Moon, J. Liese, et al. 2015. A wave of regulatory T cells into neonatal skin mediates tolerance to commensal microbes. *Immunity.* 43:1011–1021. <https://doi.org/10.1016/j.immuni.2015.10.016>
- Schietinger, A., and P.D. Greenberg. 2014. Tolerance and exhaustion: defining mechanisms of T cell dysfunction. *Trends Immunol.* 35:51–60. <https://doi.org/10.1016/j.it.2013.10.001>
- Schwartz, R.H. 1997. T cell clonal anergy. *Curr. Opin. Immunol.* 9:351–357. [https://doi.org/10.1016/S0952-7915\(97\)80081-7](https://doi.org/10.1016/S0952-7915(97)80081-7)
- Schwartz, R.H. 2003. T cell anergy. *Annu. Rev. Immunol.* 21:305–334. <https://doi.org/10.1146/annurev.immunol.21.120601.141110>
- Telander, D.G., E.N. Malvey, and D.L. Mueller. 1999. Evidence for repression of IL-2 gene activation in anergic T cells. *J. Immunol.* 162:1460–1465.
- Thornton, A.M., and E.M. Shevach. 1998. CD4⁺CD25⁺ immunoregulatory T cells suppress polyclonal T cell activation in vitro by inhibiting interleukin 2 production. *J. Exp. Med.* 188:287–296. <https://doi.org/10.1084/jem.188.2.287>
- Tinoco, R., F. Carrette, M.L. Barraza, D.C. Otero, J. Magaña, M.W. Bosenberg, S.L. Swain, and L.M. Bradley. 2016. PSGL-1 Is an Immune Checkpoint Regulator that Promotes T Cell Exhaustion. *Immunity.* 44:1470. <https://doi.org/10.1016/j.immuni.2016.05.011>
- Tomura, M., N. Yoshida, J. Tanaka, S. Karasawa, Y. Miwa, A. Miyawaki, and O. Kanagawa. 2008. Monitoring cellular movement in vivo with photoconvertible fluorescence protein “Kaede” transgenic mice. *Proc. Natl. Acad. Sci. USA.* 105:10871–10876. <https://doi.org/10.1073/pnas.0802278105>
- Tomura, M., T. Honda, H. Tanizaki, A. Otsuka, G. Egawa, Y. Tokura, H. Waldmann, S. Hori, J.G. Cyster, T. Watanabe, et al. 2010. Activated regulatory T cells are the major T cell type emigrating from the skin during a cutaneous immune response in mice. *J. Clin. Invest.* 120: 883–893. <https://doi.org/10.1172/JCI40926>
- Townsend, M.J., P.G. Fallon, D.J. Matthews, H.E. Jolin, and A.N. McKenzie. 2000. T1/ST2-deficient mice demonstrate the importance of T1/ST2 in developing primary T helper cell type 2 responses. *J. Exp. Med.* 191: 1069–1076. <https://doi.org/10.1084/jem.191.6.1069>
- Trapnell, C., A. Roberts, L. Goff, G. Pertea, D. Kim, D.R. Kelley, H. Pimentel, S. L. Salzberg, J.L. Rinn, and L. Pachter. 2012. Differential gene and transcript expression analysis of RNA-seq experiments with TopHat and Cufflinks. *Nat. Protoc.* 7:562–578. <https://doi.org/10.1038/nprot.2012.016>
- Vanasek, T.L., S.L. Nandiwada, M.K. Jenkins, and D.L. Mueller. 2006. CD25⁺Foxp3⁺ regulatory T cells facilitate CD4⁺ T cell clonal anergy induction during the recovery from lymphopenia. *J. Immunol.* 176:5880–5889. <https://doi.org/10.4049/jimmunol.176.10.5880>
- Vignali, D.A., L.W. Collison, and C.J. Workman. 2008. How regulatory T cells work. *Nat. Rev. Immunol.* 8:523–532. <https://doi.org/10.1038/nri2343>
- Wherry, E.J. 2011. T cell exhaustion. *Nat. Immunol.* 12:492–499. <https://doi.org/10.1038/ni.2035>
- Wherry, E.J., and M. Kurachi. 2015. Molecular and cellular insights into T cell exhaustion. *Nat. Rev. Immunol.* 15:486–499. <https://doi.org/10.1038/nri3862>
- Xing, Y., and K.A. Hogquist. 2013. T-cell tolerance: central and peripheral. In *Immune Tolerance*. D. Mathis, and A. Rudensky, editors. Cold Spring Harbor Press, Cold Spring Harbor, NY. pp. 15–29.
- Yang, S., N. Fujikado, D. Kolodin, C. Benoist, and D. Mathis. 2015. Immune tolerance. Regulatory T cells generated early in life play a distinct role in maintaining self-tolerance. *Science.* 348:589–594. <https://doi.org/10.1126/science.aaa7017>
- Zheng, Y., Y. Zha, G. Driessens, F. Locke, and T.F. Gajewski. 2012. Transcriptional regulator early growth response gene 2 (Egr2) is required for T cell anergy in vitro and in vivo. *J. Exp. Med.* 209:2157–2163. <https://doi.org/10.1084/jem.20120342>

Supplemental material

Tuncel et al., <https://doi.org/10.1084/jem.20182002>

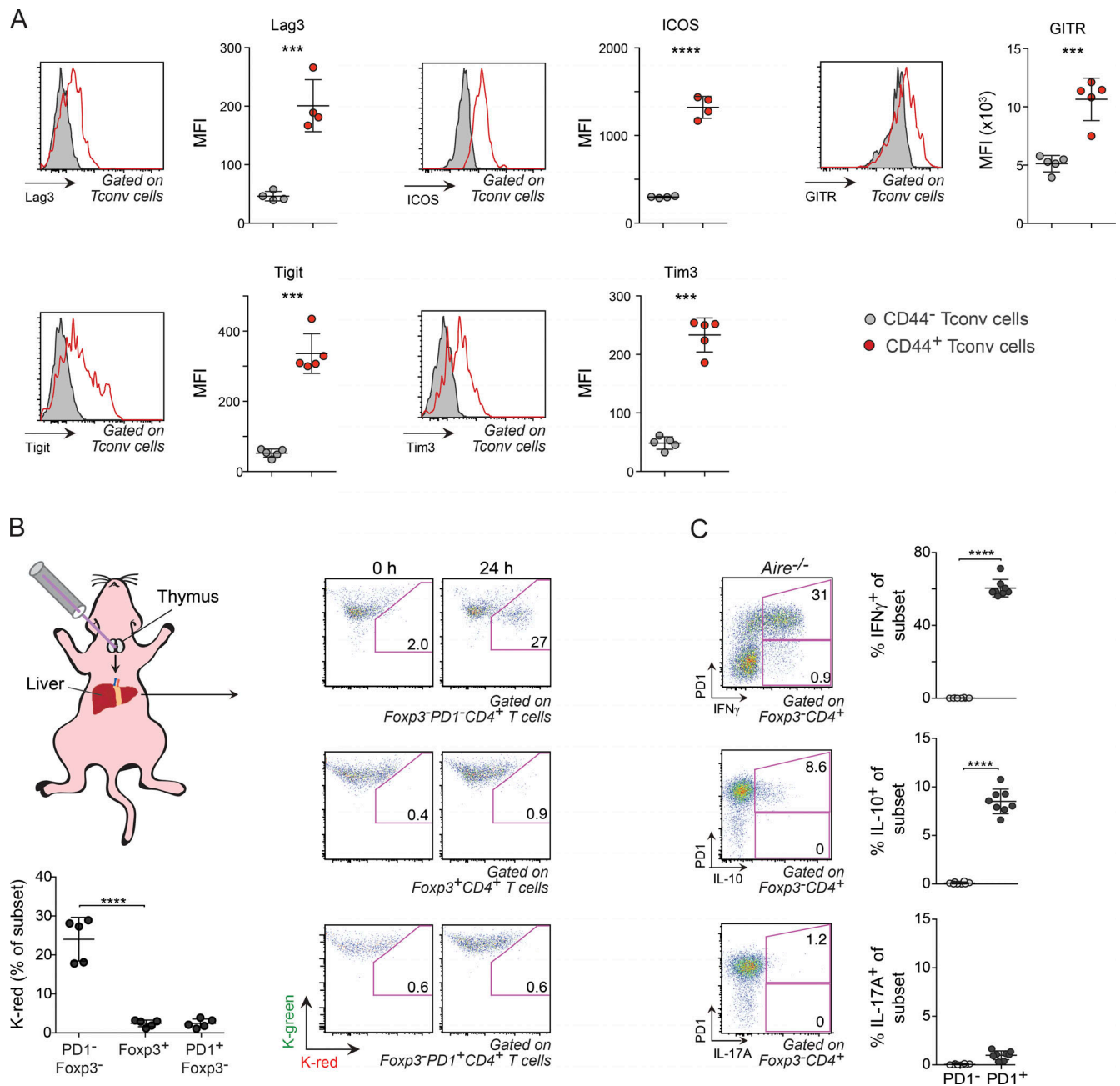


Figure S1. **Phenotype and origin of effector T cells in liver of *Aire*^{-/-} perinates.** (A) Expression of signaling and costimulatory receptors on perinatal liver CD44⁺ T conv cells. Representative histograms and summarizing mean fluorescence intensity (MFI) data from flow cytometric analyses of liver T conv cells from 12-d-old *Aire*^{-/-} mice (*n* = 4 mice/group). (B) Naive T conv cells constituted the majority of newly exported CD4⁺ thymocytes in the liver of 5-d-old mice. Thymocytes were tagged in 4-d-old *Kaede*/B6.*Aire*^{-/-} mice through light exposure. 24 h later, the proportion of tagged (photoconverted) CD4⁺ T cells was determined in the liver. Right: Pseudocolor plots show representative examples of photoconverted naive (PD-1⁻) T conv cells, Foxp3⁺ cells, and PD-1⁺ T conv cells. Bottom: Summary of frequency data (*n* = 5 mice/group). (C) Cytokine production by PD-1⁻ and PD-1⁺ liver T conv cells. Flow-cytometric pseudocolor plots and summary data of IFN γ ⁺, IL-10⁺, and IL-17A⁺-producing T conv cells from the liver of 8-d-old *Aire*^{-/-} mice (*n* = 8 mice/group). Data are pooled from at least two independent experiments. Data are shown as mean \pm SD. ***, *P* \leq 0.001; ****, *P* \leq 0.0001 (Student's *t* test).

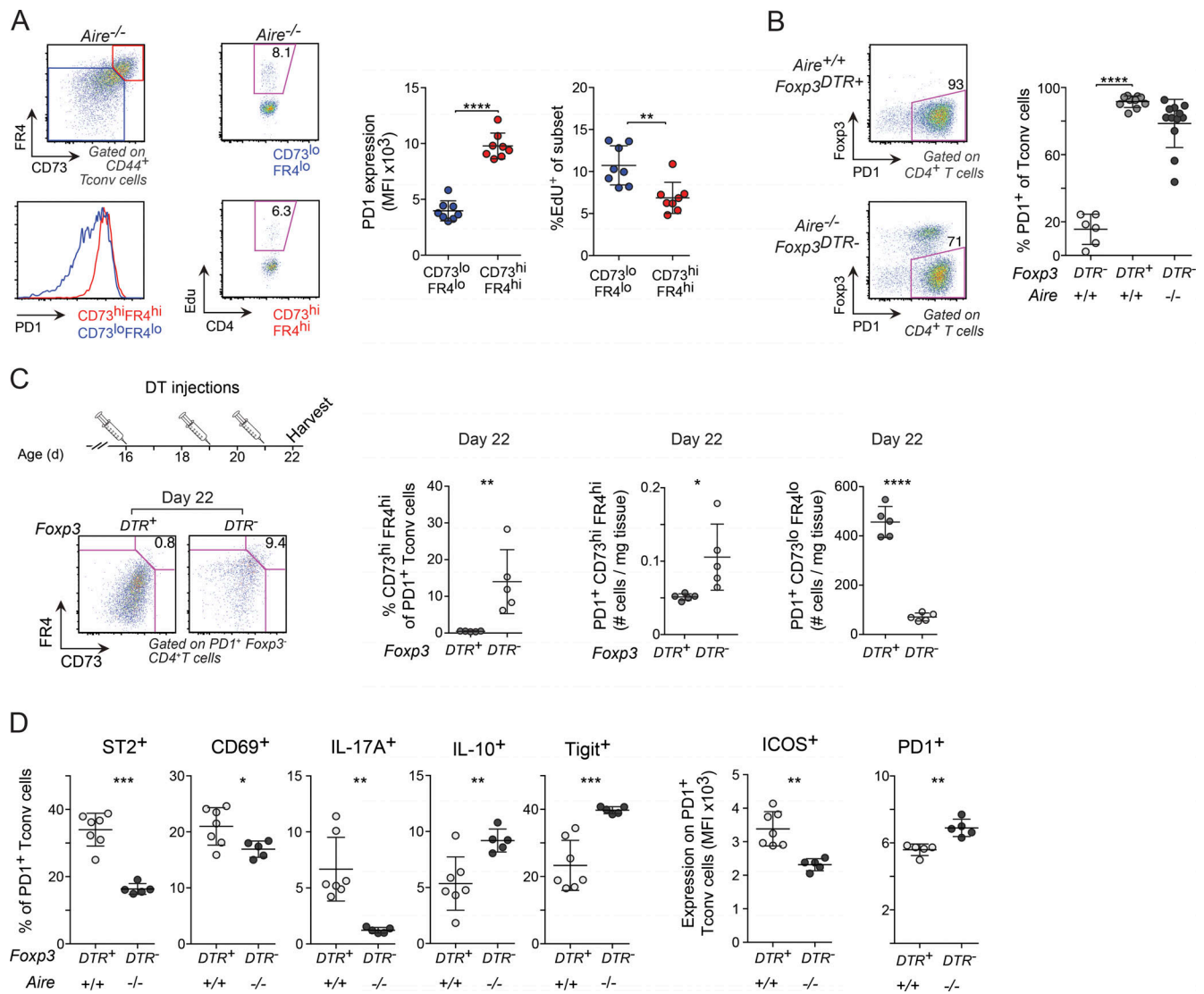


Figure S2. **Phenotypes of effector and anergic cells in *Aire*^{-/-} and T reg cell-depleted perinates.** (A) Upper left: Gating strategy of anergic (red) and effector (blue) CD44⁺ T conv cells from the liver of 10-d-old *Aire*^{-/-} mice. Lower left: Representative histogram of PD-1 expression. Center left: Representative flow-cytometric plots with gates depicting proliferating (Edu⁺) effector (top) and anergic (bottom) cells in liver from 12-d-old *Aire*^{-/-} mice, analyzed 4 h after Edu injection. Center and far right: Summary of PD-1 mean fluorescence intensity (MFI) and percentage Edu⁺ cells ($n = 8$ mice/group). (B) Frequency of PD-1⁺ T conv cells in the liver of 10-d-old *Foxp3*^{DTR+} and *Foxp3*^{DTR-} perinates after treatment with DT on days 3, 5, and 7 after birth. Left: Representative flow-cytometric plots of CD4⁺ T cells. Right: Summary of percentage PD-1 ($n = 6-12$ mice/group). (C) Frequency and number of anergic and effector cells in T reg cell-depleted perinates. Upper left: Treatment regimen for DT injection. Bottom left and right: Representative flow-cytometric plots and summary data ($n = 5$ mice/group). (D) PD-1⁺ T conv cells in T reg cell-depleted perinates were phenotypically distinct from PD-1⁺ T conv cells in *Aire*^{-/-} mice. Frequencies of cytokine- (after stimulation with phorbol myristate acetate and ionomycin) and cell surface-expressing liver PD-1⁺ T conv cells of 10-d-old *Aire*^{+/+}*Foxp3*^{DTR+} and *Aire*^{-/-}*Foxp3*^{DTR-} mice (treated with DT as in B) as determined by flow cytometry ($n = 5-7$ mice/group). Data are pooled from at least two independent experiments and show mean \pm SD. Statistical analyses as in Fig. S1. *, $P \leq 0.05$; **, $P \leq 0.01$; ***, $P \leq 0.001$; ****, $P \leq 0.0001$.

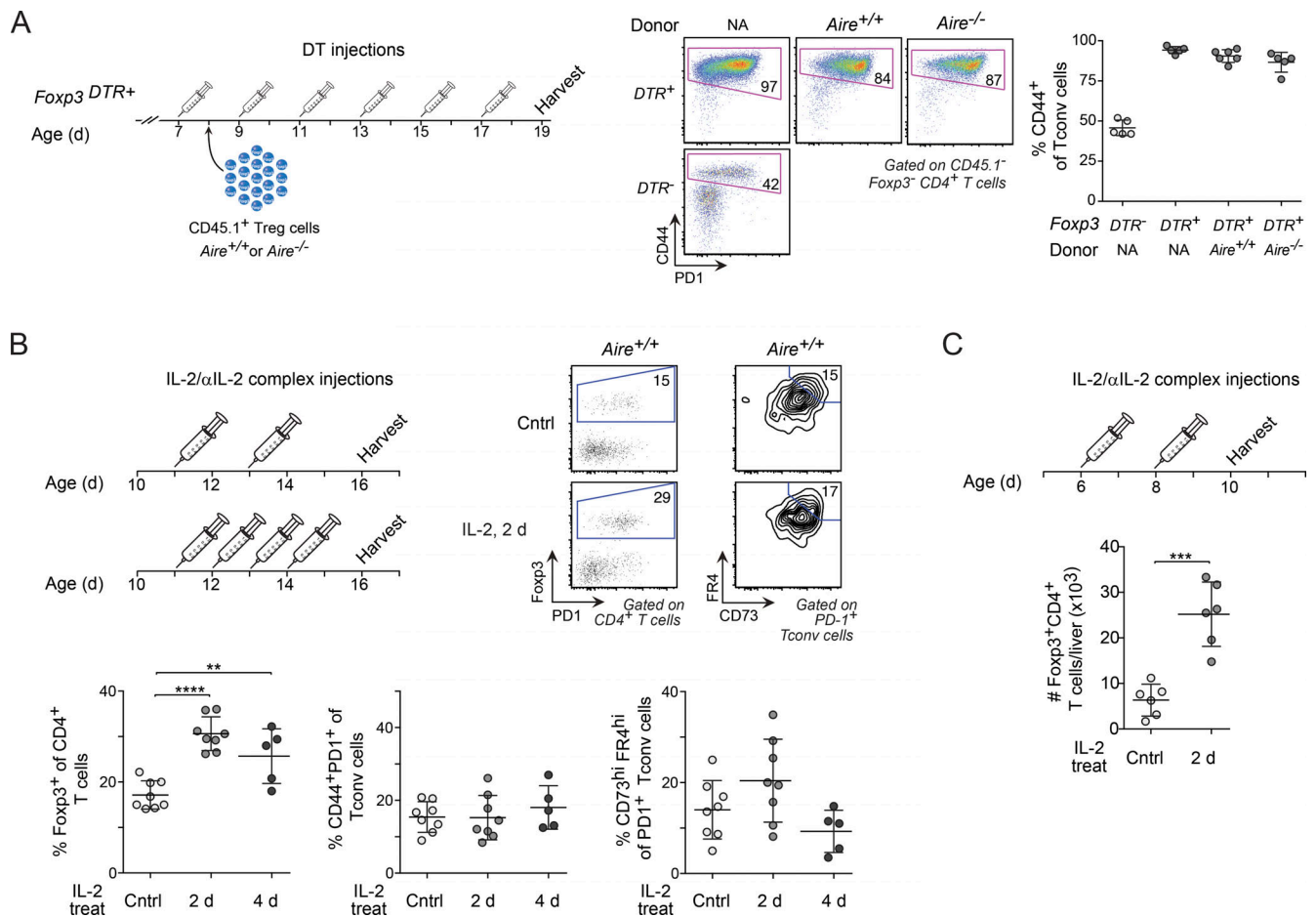


Figure S3. **Impact of T reg cells on effector cell differentiation and the abundance of anergic cells in the perinatal liver. (A)** Frequency of CD44⁺ T conv cells. Left: Regimen for adoptive T reg cell-transfer and DT treatment. Right: Representative flow-cytometric plots and summary data ($n = 5-6$ mice/group). **(B)** Treatment with IL-2 increased the number of T reg cells in the liver without affecting the proportion of anergic cells. *Aire*^{+/+} mice were treated with low doses of IL-2/anti-IL-2 mAb complexes daily or every second day between days 11 and 14 after birth, after which the proportions of various CD4⁺ T cell subsets (as indicated) were determined on day 16. Upper left: Treatment regimen. Upper right: Representative flow-cytometric dot and contour plots of total CD4⁺ T cells and PD-1⁺ T conv cells in treated and control (vehicle alone) mice. Bottom: Summary data for percentages of T reg cells, CD44⁺PD-1⁺ T conv cells, and anergic cells ($n = 5-8$ mice/group). **(C)** Number of T reg cells in 10-d-old *Aire*^{+/+} mice after two injections of IL-2/anti-IL-2 mAb complexes on days 6 and 8 after birth (using the same dose of cytokine/antibodies as in B; $n = 6$ mice/group). Data are pooled from at least two independent experiments and show mean \pm SD. Statistical analyses as in Fig. S1. **, $P \leq 0.01$; ***, $P \leq 0.001$; ****, $P \leq 0.0001$.

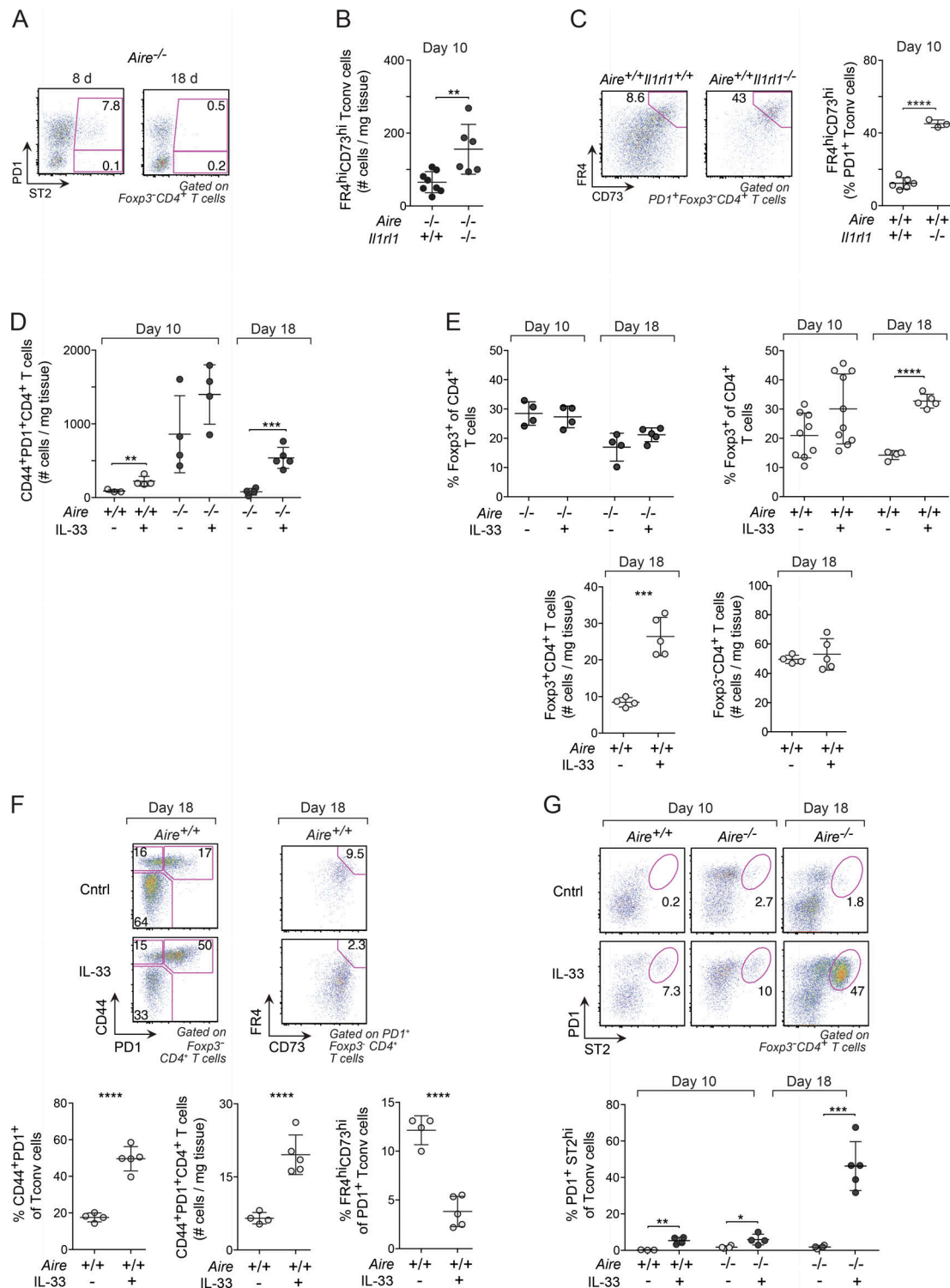


Figure S4. IL-33 inhibited anergy but promoted T reg cell proliferation and ST2 expression by liver T conv cells. (A) Representative flow-cytometric plots of T conv cells from 8-18-d-old *Aire*^{-/-} mice (see Fig. 7 A for summary data of ST2⁺PD1⁻ and ST2⁺PD1⁺ frequencies). (B and C) Impact of ST2 deficiency on the number (*n* = 6-8 mice/group; B) and frequency (*n* = 3-6 mice/group; C) of anergic cells in 10-d-old *Aire*^{-/-} (B) and *Aire*^{+/+} mice (C). (D) Number of CD44⁺PD1⁺ T conv cells after treatment with rIL-33 (see Fig. 7 E for treatment regimen). Days 10 and 18, as indicated on top of the scatter plots, represent the days of harvest (*n* = 4-5 mice/group). (E) Frequency and number of liver T reg cells in mice treated with rIL-33. Top: Frequency of T reg cells in *Aire*^{-/-} (left) and *Aire*^{+/+} (right) mice (treated with rIL-33 as in Fig. 7 E). Bottom: Number of T reg cells (left) and T conv (right) cells in *Aire*^{-/-} mice treated with rIL-33 (*n* = 4-10 mice/group). (F) Impact of rIL-33 treatment on total and anergic liver CD44⁺PD1⁺ T conv cells in 18-d-old *Aire*^{+/+} mice (*n* = 4-5 mice/group; see Fig. 7 E for treatment regimen). (G) Frequency of ST2⁺ T conv cells in mice treated with rIL-33. Top: Representative flow-cytometric plots. Bottom: Summary data (*n* = 3-5 mice/group). Data are pooled from at least two independent experiments and show mean ± SD. Statistical analyses as in Fig. S1. **, *P* ≤ 0.01; ***, *P* ≤ 0.001; ****, *P* ≤ 0.0001.

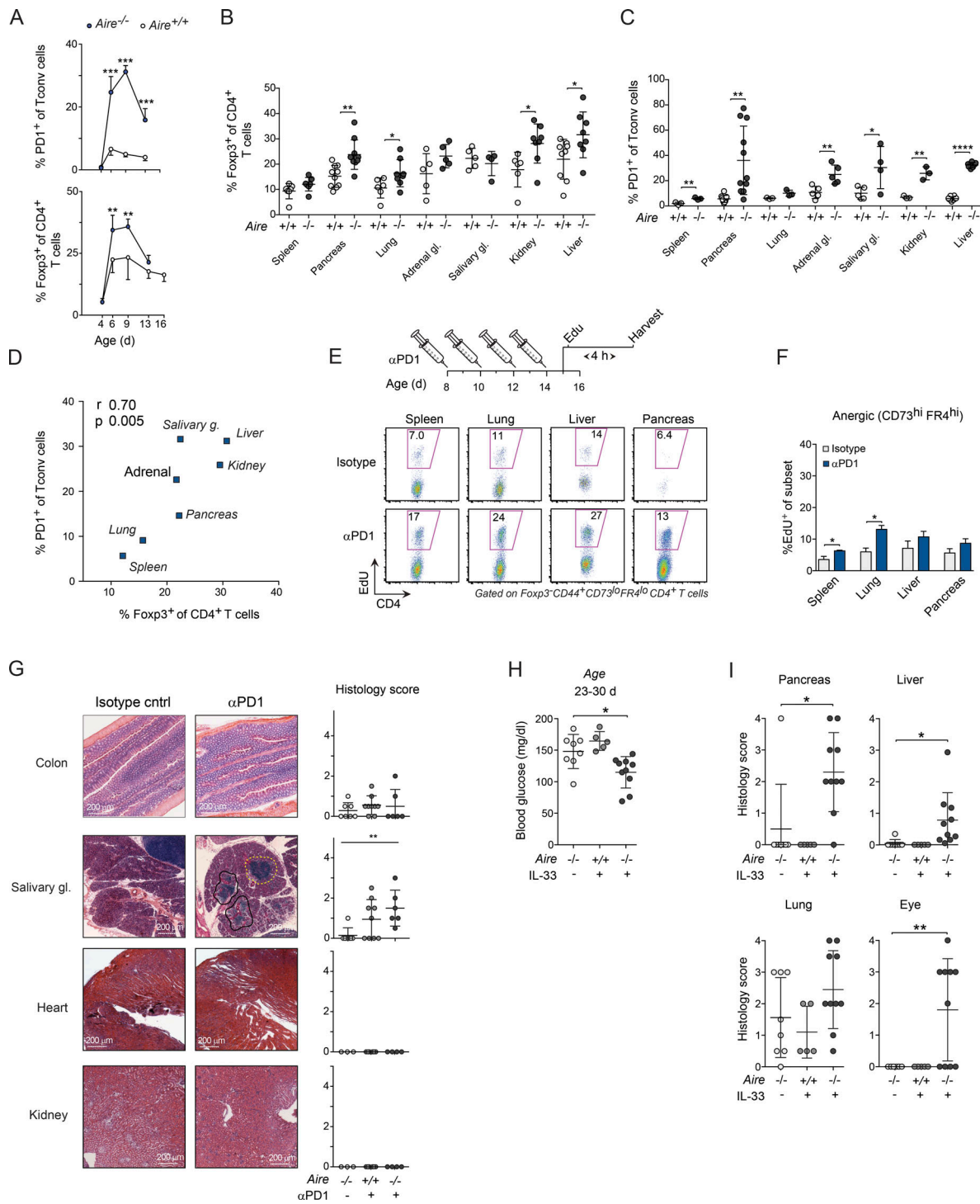


Figure S5. Impact of inhibiting PD-1 or stimulating ST2 signaling on T cell proliferation and autoimmunity in NOD perinates. (A–D) PD-1⁺ T conv cells were enriched in several nonlymphoid organs of NOD.*Aire*^{-/-} perinates. **(A)** Frequencies of PD-1⁺ T conv cells (top) and T reg cells (bottom; gated as in Figs. 1 C and 2 A, respectively) from liver of NOD.*Aire*^{-/-} and *Aire*^{+/+} littermates of various ages (*n* = 4–9 mice/group). **(B and C)** Proportions of T reg (B) and PD-1⁺ T conv (C) cells in the spleen and nonlymphoid organs of 8–10-d-old NOD.*Aire*^{-/-} and *Aire*^{+/+} littermates (*n* = 3–11 mice/group). **(D)** Correlation between frequencies of T reg cells (x axis) and PD-1⁺ T conv cells (y axis) in the spleen and nonlymphoid organs of 8–10-d-old NOD.*Aire*^{-/-} mice (median values of data shown in B and C; *n* = 3–9 mice/group). **(E)** Proliferation of CD44⁺CD73^{lo}FR4^{lo} T conv cells from various organs of 15-d-old NOD.*Aire*^{-/-} mice treated with an αPD-1 blocking mAb (or an isotype-matched control mAb) between days 8 and 14 after birth. Cells were analyzed 4 h after EdU injection (data are summarized in Fig. 9 A). **(F)** Corresponding summary data (as in Fig. 9 A) for cells with an anergic phenotype (gated as in Fig. 5 A; *n* = 3–6 mice/group). **(G)** Data from the same experiment as that depicted in Fig. 9, C and D (*n* = 6–9 mice/group). Scale bars, 200 μm. **(H)** Blood-glucose levels in NOD.*Aire*^{-/-} mice treated with rIL-33 as compared with controls (vehicle treated; *n* = 5–10 mice/group). **(I)** Histological scores related to data depicted in Fig. 9 E (*n* = 5–10 mice/group). Data are pooled from at least two independent experiments and show mean ± SD. Statistical analyses as in Fig. S1. *, *P* ≤ 0.05; **, *P* ≤ 0.01; ***, *P* ≤ 0.001; ****, *P* ≤ 0.0001.